# Abstract

# Design and Application of Multiscale Double-layered Microfluidic Device for Multi-cellular Co-culture

**Soojung Oh**

**School of Mechanical and Aerospace Engineering**

**The Graduate School**

**Seoul National University**

In this thesis, we propose about designing new microfluidic device to culture microvessel in three-dimensional space and suggest methods to analyze microvessel behavior to external condition. The device have cell culture region both in horizontal and vertical direction providing in vivo like culture condition among cells. Mainly the devices are made in flexible polymer PDMS (polydimethylsiloxane) and composed with two-layered microchannel with thin porous membrane in between. Considering the pore size of the membrane is important because it can vary the aim of the experiment. The biggest

advantage of two-layered microchannel with porous membrane is that the device can provide both isolated region and shared region in cell culture. Cells can be cultured independently in the isolated culture region while they can also share their secreting factors and even their exclusive functions through shared region. For these reasons, there are many researches and publishes dealing cell responses using this type of microfluidic device. However, there are also limitations in fabricating methodology to provide various applications so far.

Here, we have designed two types of two-layered microfluidic culture platform which can be considered invaluable system for further experiment in the field of cell culture. Each platform have an individual aim respectively; (1) Platform #1: we have established self-assembled microvessel network and analyzed microvessel damage by treating with toxic chemical; (2) Platform #2: we have observed microvessel behavior by co-culturing with cancer spheroid. Both platforms provide chemical diffusion through porous membrane at the intersecting region of upper and lower microchannel. Cells in this region have more opportunity to be nourished with fresh media which have direct influence on cell viability.

The platform #1, we have precisely aligned 0.4 μm porous polyester membrane in between the layered microchannel. Upper part microchannel is designed to culture and differentiate endothelial cells into microvessel. Once the microvessel is assembled and stabilized, toxic chemical – in this case low

concentration of SDS (sodium dodecyl sulfate) – is introduced into lower part of the microchannel. As SDS molecule is tiny enough to penetrate through the porous membrane, the external side of the microvessel is exposed to the chemical instantly. According to the toxicity of the chemical, microvessel can be maintained or damaged gradually. By mixing fluorescent molecule with the chemical, we were able to observe the fluorescent molecule penetrate through microvessel wall which can be an indicator of considering vessel wall damage.

The platform #2, we have observed microvessel behavior by co-culturing with cancer spheroid. The strong point of this platform is that we were able to culture μm sized microvessel and mm sized cancer spheroid at the same time while observing the blood vessel sprouts in vertical direction as well. In the paper, we present method steps to fabricate 200 μm sized pores in 75 μm thick PDMS membrane. This micro-pore can connect upper part and lower part and also guide microvessel to sprout towards the upper part. Upper part of the device is Ø6 mm open reservoir and lower part of the device is microchannel design to culture and differentiate endothelial cells into microvessel. During microvessel development, cancer spheroid is co-cultured in the upper part of the same device. As cancer spheroid secret plenty of growth factors to induce formation of the microvessel, we were able to observe thicker microvessel growth in the presence of cancer spheroid.

With the platform #2, we also tested selective flow by flowing two types of

fluorescent dye through upper and lower part of the device. As lower part is the region where the microvessel is assembled, dye introduced in lower part can flow through microvessel lumen while dye introduced in upper part can access through micropore to external side of the vessel. In this way, microvessel can experience different types of media supply at inner-and external side of the blood vessel barrier, which is usual condition for blood vessels in vivo. This condition realized in vitro is meaningful because selecting media is very important element to co-culture two types of different cells in one system.

To conclude, in order to fully develop the in vitro culture condition close to in vivo, we need to consider not only the cell types but also the spatial relevance among them. Reminding that our designed platform provide horizontal and vertical co-culture, most of the three-dimensional culture condition can be demonstrated in the device. Our development enables to overcome the difficulties experienced so far with existing devices and offers opportunity to design various experimental concepts in the field of microfluidic bioengineering.

**Keywords: Microfluidics; Multiscale cell co-culture; Microvessel; Toxicity test; Capillary bed**

**Student Number: 2012-30923**

# Contents


**1 Introduction ····· 15**

**1.1 Microfluidics in cell biology ····· 15**

**1.1.1 In vivo and in vitro cell culture ····· 15**

**1.1.2 Microfluidics in cell biology ····· 16**

**1.1.3 Organ-on-a-chip and importance of blood vessel····· 18**

**1.2 Aim of the paper ····· 20**

**2 Platform #1 : Double-layered microfluidic device for chemical irritancy test ····· 22**

**2.1 Introduction ····· 22**

**2.1.1 Cosmetics and dermatology ····· 22**

**2.1.2 Animal testing ban in cosmetic markets ····· 23**

**2.1.3 Alternative testing tools and challenges ····· 24**

**2.1.4 Aim of the paper ····· 26**

**2.2 Materials and Methods ····· 29**

**2.2.1 Photolithography and soft lithography ····· 29**

**2.2.2 Device design and fabrication ····· 30**

**2.2.3 Experiment set up ····· 31**

2.2.4 Cell culture ····· 33
2.2.5 Nuclei staining ····· 33
2.2.6 Chemical preparation ····· 34
2.2.7 Imaging and data analysis ····· 34
2.3 Results and Discussion ····· 35
2.3.1 Perfusable microvessel formation in the device ····· 35
2.3.2 FITC absolve and intensity difference ····· 38
2.3.3 Effect of 1% SDS ····· 40
2.3.4 Effect of SDS according to concentration ····· 43
2.4 Conclusion ····· 47

3 Platform #2 : “Open top” Two-layered Micropore Device to form Capillary Bed in vitro ····· 49
3.1 Introduction ····· 49
3.1.1 Embryology; the spatial relevance among cells ····· 49
3.1.2 Tissue engineering and blood vessel ····· 50
3.1.3 Blood vessel formation in microfluidic device ····· 51
3.1.4 Aim of the device ····· 52
3.2 Materials and Methods ····· 55
3.2.1 Photolithography and soft lithography ····· 55

3.2.2 Device design and fabrication ····· 56
3.2.3 Cell culture ····· 57
3.2.4 Culturing U87MG spheroid ····· 58
3.2.5 Cell loading ····· 58
3.2.6 Immunostaining ····· 59
3.3 Results and Discussion ····· 62
3.3.1 Microvessel formation in the open top microfluidic device ····· 62
3.3.2 Microvessel formation according to channel width ····· 64
3.3.3 Selective fluid delivery to intra- and extra-luminal side of the microvessel ····· 66
3.3.4 Culturing cancer spheroid on top of the vascular network ····· 73
3.3.5 Blood vessel recruitment ····· 77
3.3.6 Vertical angiogenesis towards cancer spheroid ····· 84
3.4 Conclusion ····· 87

4 Micro Blood Vessel Module (μBVM) for Organ-on-a-Chip Applications ····· 90
4.1 Introduction ····· 90
4.1.1 Circulatory system and human-on-a-chip ····· 90
4.1.2 Idea of hydrogel loop insert ····· 91
4.1.3 Aim of the paper ····· 92

4.2 Materials and Methods ····· 93
4.2.1 Fabrication of the microchannel ····· 93
4.2.2 Cell Culture ····· 93
4.2.3 LF–hydrogel loop preparation ····· 94
4.2.4 Live/dead assay ····· 95
4.2.5 Preparation of μBVM ····· 95
4.2.6 Immunostaining and imaging of the capillary ····· 97
4.3 Results and Discussion ····· 98
4.3.1 Loop–hydrogel culture of the lung fibroblast in μBVM ·· 98
4.3.2 Verification of blood vessel formed in μBVM ····· 100
4.3.3 Extended μBVM for Organ-on-a chip ····· 103
4.4 Conclusion ····· 105

5 Conclusion ····· 106

6 Reference ····· 109

# List of Figures

**Figure 2.1** Lists of in vitro models to replace animal tests which is approved from OECD. (Lists referenced from TSAR: tracking system for alternative test methods review, validation and approval in the context of EU regulations on chemicals. http://tsar.jrc.ec.europa.eu/)

**Figure 2.2** Comparison between HET-CAM and Platform#1. (A) Steps to perform HET-CAM. After dropping reagent, vessel morphology is observed by time. Hemorrhage, lysis and coagulation. (B) Platform #1 features similar context with HET-CAM. Red dye is upper channel where blood vessel is assembled and blue dye injected with syringe is chemical. Micro vessel is damaged by delivered chemical and observed with microscope.

**Figure 2.3** Scheme of experiment design. (A) Each layers of the device is introduced with figure. (B) Cross section scheme of the device. Width of the microvessel channel is 1.5 mm and chemical channel is 1 mm. Chemical channel overlaps under microvessel channel and deliver molecules through porous membrane. (C) Experimental setup. Inlet of lower channel is connected with tube and injected with syringe.

**Figure 2.4** Formation of perfusable microvessel. (A) Bright field image of the established in vitro microvessel. Micropost arrays provide the stable interaction between ECs and LFs resulting assembly of perfusable microvessel. (B) 7 μm microbeads (RFP) are injected in the interior of the microvessel while FITC-dye is accessed through lower channel.

**Figure 2.5** Visualizing the exposure of chemical compound to microvessel with FITC dye (332 Da) (a) FITC dye is injected through lower channel and observed with confocal microscope, 0 min. Bright green indicate the exterior

side of the microvessel while dark area is the interior side of the microvessel. After 10 min, FITC molecule is uniformly absorbed by EC cells representing molecule accessibility to microvessel through porous membrane. (b) FITC intensity change is measured by the time. FITC intensity seem to decrease along the time in exterior part while the microvessel wall have the opposite value. Also, interior part of the microvessel have no significant change meaning that the microvessel is well functioning as physical barrier resulting fluidic isolation.

**Figure 2.6** Before chemical treatment, vessel is in healthy condition. After 30 seconds exposed to 1% SDS, damage of vessel wall is clearly observed.

**Figure 2.7** Real-time observation of the effect of 1% Sodium dodecyl sulfate (SDS) to microvessel. We have tested our platform with 1% SDS solution to observe the microvessel morphology in real-time. Nuclei were stained to visualize the cell damage and we could notice that unexposed part is relatively viable

**Figure 2.8** Distinguishable result among compounds. (A) The platform is tested with 0%, 0.1% and 1% SDS. (B) Images are captured at intervals of 2.5 seconds. Each horizontal line pixel represent the time interval, 2.5 seconds. We can observe no change in 0%, starting to leak at 1 minute exposure to 0.1% SDS and immediate leak to 1% SDS.

**Figure 2.9** Intensity difference graph according to time is measured from the data 0%, 0.1% and 1% SDS solution to healthy microvessel. 40% of maximum intensity is selected as standard intensity value point to distinguish time point among reagents.

**Figure 3.1** Scheme of capillary bed and “open-top” microfluidic device. (A) Capillary bed is complex of dense microvessel and tissue. Nutrients are supplied to tissues while blood flows through microvessel, from arteriole to

venule. (B) The device features similar structure with capillary bed. When blood vessel is assembled in the channel, media can flow from one channel to the other. By culturing cell spheroid in the reservoir, cells can experience close contact through micropore, which can enhance cell-to-cell interaction. (C) The device size can be estimated by comparing with penny. (D) Channel design. Fibrin gels are captured within micropillar walls and cells are cultured in 3D environment. Arrays of micro pores are located in the middle channel connecting upper and lower channels.

**Figure 3.2** Fabrication Procedures of micro-pore embedded microfluidics. We have made inversed PDMS pre-mold to have both micropillar and micropore in a thin membrane. By coating with Teflon, we were able to make boundaries and prevent same materials merge together. As pre-mold is featuring inversed topology, micropost become micropore and pores become pillars. Post-mold with reservoir removed is bonded and the device is ready for the next step

**Figure 3.3** (A) Design of upper and lower channel of the Platform #2. (B) Method steps to co-culture vascular network and cancer spheroid. (C) Method steps to induce angiogenesis co-cultured with cancer spheroid.

**Figure 3.4** (A) Formation of microvessel in an open-top micropore device. We have observed endothelial cells assembling each other day by day. (B) To visualize the microvessel formation, cells are stained with CD31 and nuclei. FITC dye can flow inner lumen while microvessel is alive.

**Figure 3.5** Micropore device is compared with control. Fresh media can be delivered to center channel through micropore so culture condition ca be enhanced. Compared to control, we were able to observe that in the micropore channel, blood vessel can be linked well and have perfusable lumen. The control, even though cells are alive, we were not able to observe any lumens.

**Figure 3.6** (A) After blood vessels are fully developed in a micropore channel, we have flowed red dye through the outer reservoir and green dye through center reservoir. Red dye can flow inside the inner blood vessel and green dye can access exterior side of blood vessel. (B) The dye intensity graph clearly shows opposite peak where blood vessel wall stands. (C) This condition has maintained for 30 minutes.

**Figure 3.7** (A) Four sets of experiment media combination is listed. (B) We have cultured microvessel in different media condition for two days. Yellow arrow in EGM-EGM sample indicate the difference in vessel diameter. Ten vessels are measured from each sample.

**Figure 3.8** We were able to experience difference in vessel diameter. With the original medium condition, vessel wall grew about 50% larger. When the medium is different in upper and lower channel, vessel experienced little growth or sustained. When we used the medium which is not for EC culture, vessel shrank or degraded.

**Figure 3.9** Toxicity test can be performed with Platform #2 as well. Rhodamin-Dextran in filled inside the lumen. When SDS solution spread down through micro pore, vessel wall start to leak at time 24s.

**Figure 3.10** (A) After blood vessels start to make vessels in a micropore channel, we have loaded cancer spheroid (U87MG) on top of the micropore. Cancer spheroid are about 400 ~ 500 μm large. The pores are designed in several sizes. (B) Immuno-stained micro vessel. We have observed cross-section of the blood vessel. Cancer cells migrated downwards to microvessel right under spheroid, and covered around the microvessel. Green is endothelial cell and red is F-actin which stains both cell. However, microvessel without spheroid have more clear vision and no other cells surrounding blood vessel.

**Figure 3.11** (A) Four sets of cell combination (LF/Spheroid). First two images both have LFs mixed with vessel and only the first one is co-cultured with spheroid. Next two images are without LFs and third image is co-cultured with spheroid. (B) By comparing the vessel width, Spheroid can enhance the growth of vessel diameter. From the figure, LFs affected connectivity.

**Figure 3.12** (A) Vascular network with and without cancer spheroid showed difference in their growth. (B) We have measured intensity of CD31 where micro pores overlap. Micro pores around spheroid had higher intensity value compared to the pores far from spheroid.

**Figure 3.13** HDMEC is attached on a hydrogel wall and angiogenesis is induced by LFs and U87MG spheroid. Faster growth of microvessel sprouts are observed near cancer spheroid.

**Figure 3.14** Yellow dotted line indicate where the spheroid is and microvessel lumen are thick enough to flow green dyes right underneath the spheroid. Position 1 is immuno-stained microvessel with CD31. Clear lumen and vessel sprouts vertically directed is observed. Position 2 is cross section image of microvessel filled with FITC-dextran. Dyes are observed filling vertical sprout direction.

**Figure 4.1** Schematic showing the preparation of a hydrogel loop. The figure showes each steps to prepare hydrogel loop. Loop is trimmed from conventional cell spreader and premixed hydrogel containing cells are pipetted inner surface of the loop. Hydrogel loop is incubated in the 96 well before use. Each loop is inserted into reservoir of the device secreting growth factor. Hydrogel boundaries prevent cells from crawling out of the loop. Hydrogel loop can be freely removed or exchanged with other loop.

**Figure 4.2** Live/dead assay is performed to verify cell viability. (A) Cells are

uniformly distributed within hydrogel. Loop boundary keep cell from escaping and prevent cell interference. (B) Live/dead assay is performed for cells in hydrogel loop. Cells are well cultured during 10 days in vitro. Nuclei of the cells are reconstructed with IMARIS and counted by their color. Blue sphere stands for live cells while red sphere are dead cells. (C) Graph shows that a high percentage of cells (95%) remains viable within the gel for up to 10 days referring no significant difference to DIV 1.

**Figure 4.3** (A) Bright-field images of HUVECs forming a capillary vessel inside of the microchannel were captured from day to day. Morphology of the HUVEC is observed. Maximum channel length to maintain perfusability is 2 mm. (B) Immuno-stained μBVM. μBVM is stained to visualize vessel network and interior lumen. 7 um red fluorescent beads are introduced from the reservoir to verify perfusability. Scale bar shows 50 μm.

**Figure 4.4** (A) Bright field image of connected two units of μBVM. Center insert region is allowed to insert organ representing cell types into microfluidic device with only containing micro-blood vessel. (B) Cells in Hydrogel loop can be decoupled from cells in the device after they spend enough time to affect each other. This is one of big advantage of the μBVM system. By culturing any cell types in hydrogel loop and exchange, this can be another cell secreting source.

**Figure 5.1** Advantage and disadvantage of the devices. Platform # 1, 2 is integrated from original platform and have an improved points. Important criteria is listed and each platform ability is compared.

# 1 Introduction

## 1.1 Microfluidics in cell biology

### 1.1.1 In vivo and in vitro cell culture

Both in vivo and in vitro experiments are essential to investigate and obtain detailed information about structure-function relationships in living organism. Usually their terms are defined depending on the experimental model used. In vivo experimental models include tests performed on whole living organisms; animals and humans including plants. In vivo experiments are necessary to test toxicity and immune reaction of new drugs, to reveal cause and effect of diseases, and to develop new surgical procedures. They can bring out reliable and significant data which can improve the quality of human life while they require large cost of time and finance. However, even with its advantages, there are social and ethical opinions to reduce the abuse in animal testing. There are acceptable arguments that there is a fair chance of the animal tests can be substituted with in vitro experiments.

On the contrary to in vivo models, in vitro experimental model is generally referred to the tissue and cell culture experiments processed under controlled, artificial environment outside their normal biological context. The primary advantage of in vitro experiment is that it simplifies the system under study so

that the investigators can focus on a small number of variables. Even though they fail to replicate precise cellular conditions of organisms, from its simplified system, they are usually amenable to miniaturization and automation, yielding high-throughput screening methods for testing molecules in pharmacology or toxicology. Although these methods can bring out significant experiment results, it is necessary to perform precise clinical tests because in vitro models experience huge gap between animal models.

To narrow the biological difference between two types of models, in vivo like in vitro models are developed utilized with novel engineering technologies; tissue engineering, bio-engineering, bioMEMS and organ-on-a-chips. These interesting research fields have fulfilled in developing new in vitro models close to real organisms; they can freely manipulate three dimensional culture environment instead of culturing cells in two-dimensional petri dish. To recall the fact that the cells behave differently where they anchor to, these spatially controlled environment greatly enhance the function of cells which eventually improve the outcome of experiment. Following sections will introduce novel engineering techniques to design such in vivo like in vitro models.

### 1.1.2 Microfluidics in cell biology

Microfluidics is the technology to manipulate small ($10^{-9}$ to $10^{-18}$ liters)

amounts of fluids in the designed channels less than a millimeter [1, 2]. This feature of device provides number of advantages that allows for researchers to use very small quantities of fluidic samples which directly related to low cost experiment. Small sized cross-section and relatively long microchannel develop laminar flow inside the channel which offers capabilities in the control of concentration of molecules in space and time. Moreover, the device fabricated with glass and PDMS (polydimethylsiloxane) support optically transparent vision so that it can be easily observed with various colors of dyes and possible to obtain high resolution image in the magnifiable range of microscope.

In early microfluidics history, it was used to perform molecular analysis such as chromatography and electrophoresis. The device was perfect enough to achieve high sensitivity and high resolution using very small amounts of sample. Then researchers were eager to develop more delicate applications in the field of chemistry and biochemistry based in this characters of microfluidics. Therefore emerged application designs such as valve, mixers and pumps. These novel applications gave many inspiration to design new tools to manipulate inner and external environment of the device which further lead to the development of lab-on-a-chip (LOC) technology. LOC is a device performs miniaturized laboratory functions to achieve automation and high-throughput screening on a single chip designed with microchannel and often indicated by

micro-total-analysis-systems (μTAS) as well. Because of their flexibility and simplicity, numerous designs and applications of LOC used in the field of biology have been presented throughout few decades [3, 4]. Typically we focus on the microfluidics designed to culture cells and manipulate the condition to derive model systems to represent certain physiological functions of tissues and organs. This is referred to “organ on a chip” which we will continue on following chapter.

### 1.1.3 Organ-on-a-chip and importance of blood vessel

“Organ on a chip” is one of applications from microfluidics as introduced above. We can simply compare the model system as “decent home for cells” and we can be the architect designers and engineers. It is important for us to understand the natural *in vivo* condition where cells belong and perform reconstructing new habitat for cells maintaining their key factors of original niche. Therefore cells can live happily in their new home keeping their typical cell characters and functions indeed. There are many literatures introducing and proving enhanced culture environment compared to cells cultured on cell culture dish [5-7]. As the cells behave according to where they come from, it is important to design structure considering their in vivo environment. For example, neurons live in extra-cellular matrix (ECM) mainly composed with

matrigel. And they can exchange their signal from axons. Also they are spatially oriented in complex neural network. To demonstrate these features, brain on a chip is designed to spatially control soma and axon [8]. From the device, many application models have been published to observe neural behavior [9-12]. Likewise, liver[13], kidney[14], lung[15], gut[16] and skin[17] model is proposed and many reviews are published [18, 19]. Final goal in organ on a chip is to connect these models in to one whole system called “human-on-a-chip”. There have been approaches to accomplish the goal in steps, by linking two different organ samples in one fluidic device [20, 21]. However, to understand the link and circulation of the system, it is the role of blood vessel network. In our body, blood vessel is spread in every corner in our body in appropriate thickness and cell combination. They provide paths for cells and nutrient to circulate in our body. From this, our body can maintain homeostasis and organs can interact each other. Also, as blood vessel always intimately interact with tissues and organs, there are many reactions and related disease known. Not only the organs but also how to establish and accomplish functional blood vessel in vitro is always an issue as well as designing models cultured together with tissues and organs. Therefore, many group around the world have published novel methods to culture perfusable blood vessel cells in microfluidic device and opened a new era in the potential of human on a chip [22, 23].

## 1.2 Aim of the paper

Here in this paper, we aim for a co-culture platform of perfusable blood vessel and applications. As mentioned above, blood vessel is essential to support and connect organs. Also blood vessel is related to most of biological reactions so that the appropriate in vitro model is necessary. First we introduce double-layered microfluidic device to perform toxicity test with assembled microvessel. Toxic chemical permeate through skin can arouse tissue damage which can cause second reaction in dermis; microvessel.

Second chapter we demonstrate engineered microfluidic platform to co-culture microvessel and cell spheroid. We can expect novelty of the platform from the reason that the previous designs were unable to culture small sized cell tissue within the microchannel while our device can perform completely. With the device, we have assembled microvessel according to channel length. Also we have observed vessel difference co-cultured with cancer spheroid. We were able to conclude that the cancer spheroid can attract vessel growth and influence vessel diameter.

And the last chapter we introduce method to culture micro blood vessel module (μBVM) which can be used in body-on-a-chip applications. From this method we were able to design platform #1 which is important to remove fibroblast before doing the irritancy test. Removing of certain tool is figured

similar with transwell however, hydrogel-loop is more compact and provide three dimensional cell culture. Any cells or hydrogel can be mixed within the loop which informs that this simple tool can be a great carrier containing various secreting factors.

# 2 Platform #1 : Double-layered microfluidic device for chemical irritancy test

## 2.1 Introduction

### 2.1.1 Cosmetics and Dermatology

Cosmetics is mixtures of chemical compound to enhance the appearance or odor of the human body. Cosmetic product is firstly considered as luxuries, which is not necessary for our living. However, since people are eager to decorate themselves to look more attractive, cosmetics are not just luxuries any longer. Furthermore, people are using cosmetic products as semi-medicine, expecting improvements of their body. Some products are even developed as functional cosmetics, which can protect skin and improve skin condition. Most of their purpose is to regulate melanin, dehydration and to protect from sun burn. Therefore, to develop such products, researchers is necessary to understand dermatology as well not only chemistry. However, as the product is generally applied directly on to the skin, the most important thing is to prohibit usage of toxic chemical from the ingredients so that all product can be safe and harmless. Toxic ingredients cannot be ever used and they must be fully tested before applied to human. Human skin generally evolved according to ethnic group following their own history for hundreds of years exposed to weathers in certain

region. Therefore human have distinct characters largely categorized with local. This means that to develop a products, different types of human skin condition needs to be gathered in big data and be considered in most of the condition which will generally fit to the most. However, as there have been no appropriate complex model to represent human skin so far, animals are used in the experiment. As mentioned in chapter 1.1.1, there are social and ethical opinions to reduce the abuse in animal testing. There are acceptable arguments that there is a fair chance of the animal tests can be substituted with in vitro experiments.

### 2.1.2 Animal testing ban in cosmetic markets

Researchers proceed in vivo and in vitro experiments to sort out biocompatible ingredients. Firstly they process with in vitro cell culture with petri dish. Simple and easy method to test toxicity of the product. However, in vitro tests does not perfectly compensate with in vivo result. As an animal body is multi complex whole system, one material which were fine at in vitro experiment can possibly have chance to harm the in vivo system. Cells or tissues might transform the ingredient while they metabolize which can harm the animal body. Therefore, animal testing is necessary to develop cosmetic products before used to humans. However, recent movements to ban the animal testing is appearing all around the world. Animal ethic is considered to ban the

animal testing. Their opinion is that anyhow since the cosmetics are considered as luxuries unlike medicine, abuse of testing to animals is not right. They argue that researchers have to stop the animal experiment and figure out the alternatives. These kind of campaigns have been appeared since 1993. Finally on 2013, EU made rules not only to prohibit animal testing in cosmetic development but also even not to export or import any products tested with animal. EU is the largest cosmetic market worldwide, and these kind of movement influenced all around the world. Even in Korea where were campaigns and organizations to save animals from harm. And Amorepacific group – largest cosmetic research and development company in Korea – made promise not to execute animal testing while developing new products. In these public movements lead to strong necessity of alternative testing tools which is reliable and understandable enough to verify the toxic ingredients and after all, replace animal models.

### 2.1.3 Alternative testing tools and challenges

Since it is prohibited to test on animals, OECD has validated alternative methods to replace animal tests as listed in Figure 2.1. In most of skin irritancy tests, reconstructed human skin models are used. Reconstructed human skin is a living skin which is artificially cultured and differentiated from cells dissected

from human skin [24-26]. It is tested with their viability, permeability, stiffness and further characteristics [27-30]. Although the model is not yet perfectly the same with the skin we all have, it is novel and useful enough to be accepted to public. Methods and models are well established and systemized so that commercial products are available. Episkin and MatTek is the largest skin model company and they possess many techniques, patents and advanced researchers. Models handle basically with keratinocyte from several areas of skin, dermal fibroblasts and melanocyte. Researches are still going on to successfully culture with nerve cells and blood vessel cells in order to establish closer model to our real skin [31, 32].

Also there are tests used with tissues dissected from animals. Models categorized in eye irritancy test to replace the rabbit eye tests well known as Draize test [33]; bovine corneal opacity and permeability (BCOP) [34], isolated chicken eye test (ICE), isolated rabbit eye test (IRE) and hen's egg test on the chorio-allantoic membrane (HET-CAM). They evaluate the tests comparing the corneal opacity, swelling, fluorescein retention and morphological effects by time. They have advantages that they are possible to draw out the discriminative results among tested reagents however, they also have the disadvantages that they are still an ex vivo experiments and have limitations on methods of analysis.

### 2.1.4 Aim of the paper

In this chapter, we introduce the double-layered microfluidic device designed to perform chemical irritancy test and predict outcomes. The purpose of the designing the device is to culture microvessel and suggest method to observe vessel damage according to applied chemical. The device features similar context with HET-CAM assay described on previous chapter. As the purpose of HET-CAM assay is to observe morphological changes such as blood vessel hemorrhage, lysis and coagulation after the treatment (Figure 2.2 A), we have also designed the device that can culture micro vessel and treat chemical afterwards. Upper and lower channels are designed to culture micro vessel and treat chemical respectively. In between the channels, 0.4 μm porous membrane is sandwiched to isolate each layer but to share fluids. HDMECs and LFs are cultured to establish perfusable micro vessel in the device. After the micro vessel is formed, we have treated the device with toxic material, which we have choose sodium dodecyl sulfate (SDS) for the experiment (Figure 2.2 B). SDS is mainly used in detergents such as cleaners, soap, toothpastes, shampoos and baths. As the application with SDS is intimate with human living, it is important to be used safe. We have tested SDS in several concentration to identify the effect of toxicity to micro vessel.

| Test types | Approval of Methods |
|---|---|
| **Skin Corrosion** | Transcutaneous Electrical Resistance Test (TER)<br>EpiSkin™<br>EpiDerm™<br>SkinEthic™ RHE<br>Human Epidermis Equivalent epiCS (EST1000)<br>In Vitro Membrane Barrier Test Method for Skin Corrosion (CORROSITEX) |
| **Skin Irritation** | EpiSkin™<br>EpiDerm™<br>SkinEthic™ RHE |
| **Eye Irritation** | Bovine Cornea Opacity Test (BCOP)<br>Isolated chicken eye test (ICE)<br>Isolated rabbit eye test (IRE)<br>Hen's egg test - chorio-allantoic membrane (HET-CAM test) |

**Figure 2.1** Lists of in vitro models to replace animal tests which is approved from OECD. (Lists referenced from TSAR: tracking system for alternative test methods review, validation and approval in the context of EU regulations on chemicals. http://tsar.jrc.ec.europa.eu/)

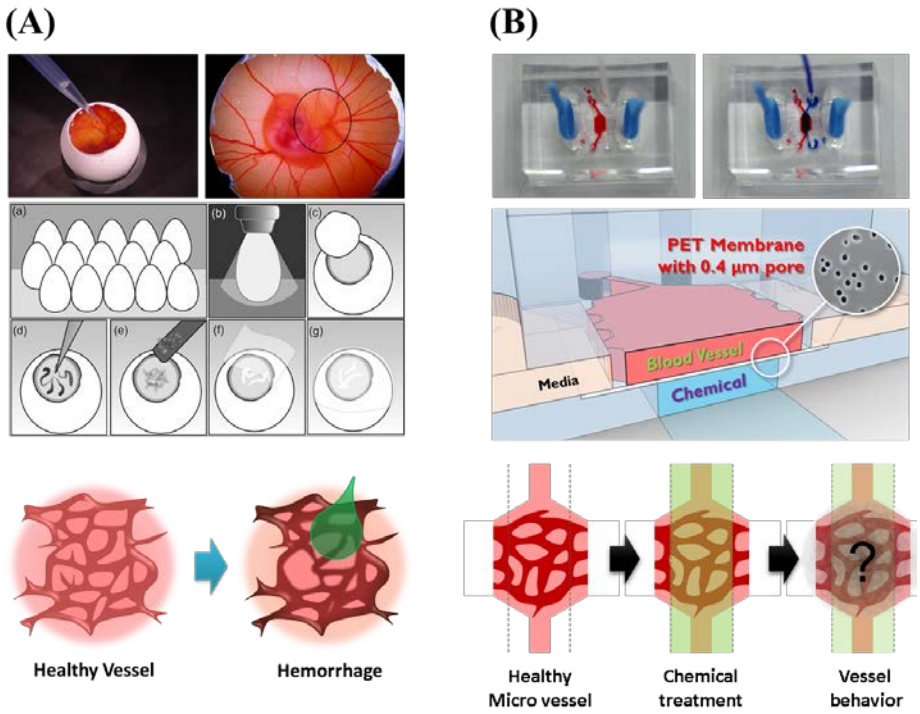


**Figure 2.2** Comparison between HET-CAM and Platform#1. (A) Steps to perform HET-CAM. After dropping reagent, vessel morphology is observed by time. Hemorrhage, lysis and coagulation. (B) Platform #1 features similar context with HET-CAM. Red dye is upper channel where blood vessel is assembled and blue dye injected with syringe is chemical. Micro vessel is damaged by delivered chemical and observed with microscope.

## 2.2 Materials and Method

### 2.2.1 Photolithography and soft lithography

Two individual film photo-mask sets are drawn with commercial CAD program (AutoCAD, DE); one is for micro vessel part and the other is chemical channel. Photolithography was processed to fabricate replicable mold. Two molds are fabricated in same manner. Prepared silicon wafer (Unisil, KR), is cleaned with plasma etcher (FEMTO Science, KR). SU-8 100 (Microchem, US) is spin-coated on a clean wafer; 150 μm thickness for micro vessel mold (30 seconds in 1750 rpm) and 100 μm thickness for chemical channel (30 seconds in 2750 rpm). Wafer is then soft-baked on a hot plate, 10 minute on 65°C and 45 minutes on 95°C continuously. Printed film photo mask (Hanalltech, KR) is then tightly contact to the surface of the wafer. UV radiation with 365 nm wavelength is exposed for the next step using conventional 500 W mercury lamp (Osram, DE) for 40 seconds (20 mW/cm$^2$, Seoungwoo MST, KR). After the exposure, wafer is post-baked on a 95°C hotplate for 10 minutes. Remaining photoresists are developed with thinner (AZ1500, KR) and designed patterns are obtained on the wafer.

PDMS (Polydimethylsiloxane, Sylgard A/B, Dowcorning, US) is used to replicate the fabricated molds. Sylgard A/B is the commercial product from Dowcorning and prepared with elastomer base and curing agent. They are

uniformly mixed in 10:1 ratio and degassed in a vacuum pump. Degassed mixture were then poured on a silicon wafer molds and baked on a 95°C hotplate. After PDMS is polymerized, it is detached on a wafer and trimmed in a right size to use.

### 2.2.2 Device design and fabrication

The device is composed with two pieces of PDMS mold and one piece porous membrane. Two pieces of PDMS is trimmed from each silicon wafer molds and polyester membrane with 0.4 μm pore and 10 μm thickness is cut out from the transwell (CA#3450, Corning, US). Upper device is designed a 1.5 mm width channel with hydrophobic micro pillar arrays to capture fibrinogen (Sigma Aldrich, US) and endothelial cell (Figure 2.3 A, B). In both side of reservoirs, hydrogel loop capturing fibroblast is inserted to secrete growth factors which is essential to endothelial cell differentiation. Hydrogel loop can be extracted after the micro vessel is assembled (detail information is described in chapter 4). It is important to remove fibroblast when observing the chemical effect to the micro vessel because if the other cell is present, they might haze the sight or secrete signal that can influence micro vessel behavior. In the middle, there is the porous membrane in suitable size to cover the interfering channel between upper and lower channels. We were able to isolate the cells as the pore size is 0.4 μm, which is smaller than usual cell size. However, fluids and molecules

can freely penetrate through the membrane. Finally, we designed lower channel with 1 mm width for chemical intrusion. From the syringe, chemical can flow through the tube into the device.

### 2.2.3 Experiment set up

After the micro vessel is assembled in the microfluidic device, hydrogel loop is decoupled and we were able to get a device only with micro vessel. Tube with 1 mm diameter is connected to inlet and outlet of lower channel. Chemical is filled in syringe and its end is connected to tube. From the syringe, chemical is injected to the device and it is transported to upper channel through porous membrane (Figure 2.3 C).

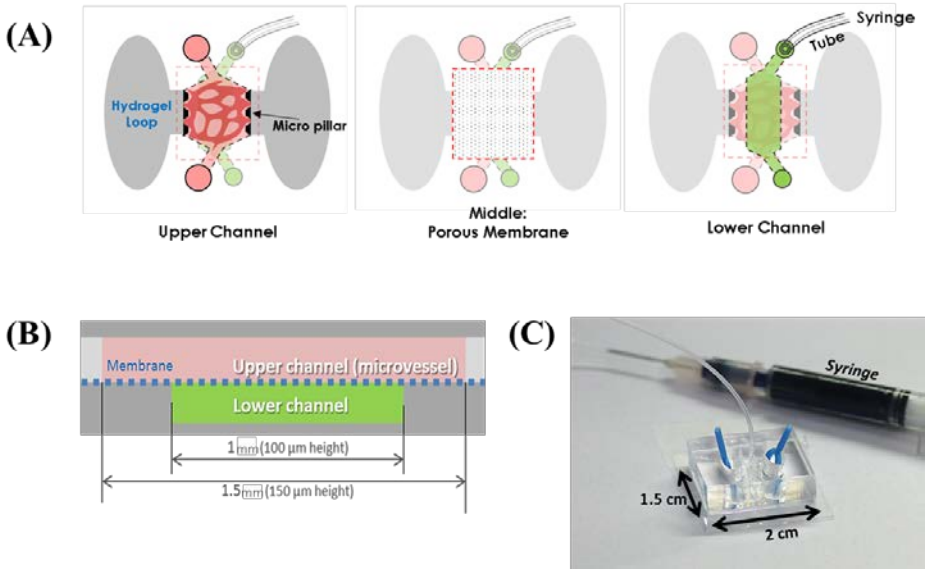


**Figure 2.3** Scheme of experiment design. (A) Each layers of the device is introduced with figure. (B) Cross section scheme of the device. Width of the microvessel channel is 1.5 mm and chemical channel is 1 mm. Chemical channel overlaps under microvessel channel and deliver molecules through porous membrane. (C) Experimental setup. Inlet of lower channel is connected with tube and injected with syringe.

### 2.2.4 Cell culture

HDMECs (Lonza, Basel, Switzerland) were cultured in the endothelial growth medium (EGM-2 MV; Lonza), and cells between passages 4 to 5 were used. Primary human LFs (Lonza) were cultured in fibroblast growth medium (FGM-2; Lonza), and passages 6 to 10 were used for the experiment. To harvest the cells, they were rinsed with phosphate buffered saline (PBS) and treated with 0.25% trypsin–EDTA (Gibco, Carlsbad, CA). After 2 min, M199 (Lonza) containing 10% fetal bovine serum was added to neutralize the effect of the enzyme. Detached cells were collected and centrifuged for 2 min in 1100 rpm, and diluted in EGM-2 to reach a certain cell number in the suspension.

### 2.2.5 Nuclei staining

To configure the physiological relevance of the blood vessel, samples were fixed with 4% paraformaldehyde. They were permeabilized with 0.15% Triton X-100 for 15 min and treated with PBS solution containing 3% bovine serum albumin (BSA; Sigma-Aldrich, St. Louis, MO). To visualize the nuclei of the blood vessel Hoechst 33342 is mixed with 3%BSA in 1:1000. Fluorescent images of the nuclei were taken with the confocal microscope.

### 2.2.6 Chemical preparation

SDS 0.1%, 1% v/v (Sigma Aldrich, US) solution is diluted in PBS and stored in room temperature. A trace of FITC (Sigma Aldrich, US) powder is mixed with SDS solution to show fluorescence. PBS is used for control and they are prepared in 1 ml syringe connected to in 1 mm diameter tube.

### 2.2.7 Imaging and data analysis

Fluorescent, time-laps and z-stack images of the device were observed with confocal microscope (Olympus FV1000, JP). 405 nm, 488 nm and 594 nm lasers were used to visualize nuclei stained with CD31, FITC dye and red fluorescence polymer beads respectively. Figures are saved in TIFF file and opened in open software ImageJ. Fluorescent intensity according to elapsed time were measured with ImageJ and drawn is graph. Also, series of figures are compressed in movie.

## 2.3 Results and Discussion

### 2.3.1 Perfusable microvessel formation in the device

We have cultured HDMEC with fibrin gel in the middle channel of the device. Micropillar can capture the gel in certain region. In the side reservoirs we have put LF-hydrogel-loop in order to secret growth factors to differentiate endothelial cells to microvessel. In 7 days in vitro, we were able to connect perfusable microvessel (Figure 2.4 A). We have tested the perfusability by introducing 7 um red polymer beads. The beads can be mixed with media and flow through channel and lumens. Microbeads were observed in inner lumen of microvessel. None of them were detected in exterior side of the lumen which means the microvessel is perfused and channels are linked with microvessel from one to the other. By imaging the device in z section, lumen filled with microbeads were constructed (Figure 2.4 B). Next we tested the device injecting FITC dye in lower channel. FITC dye were filled directly when we injected the dye with syringe. By imaging the device in z direction, we were able to see FITC molecule diffused from the lower channel to upper channel. FITC molecule exists at exterior side if the microvessel, covering surfaces. However, green signal did not measured inside the microvessel which means, the microvessel wall prohibit molecules to penetrate. Or it could mean that if they can penetrate through the microvessel wall, the inner flow of the vessel wash out the FITC molecule. In any case, microbeads and FITC dye is blocked with

microvessel wall and not mixed together. And this condition is imaged with confocal microscope. We were able to bring out the result that the device can flow inner microvessel and diffuse other material in exterior side of the microvessel.

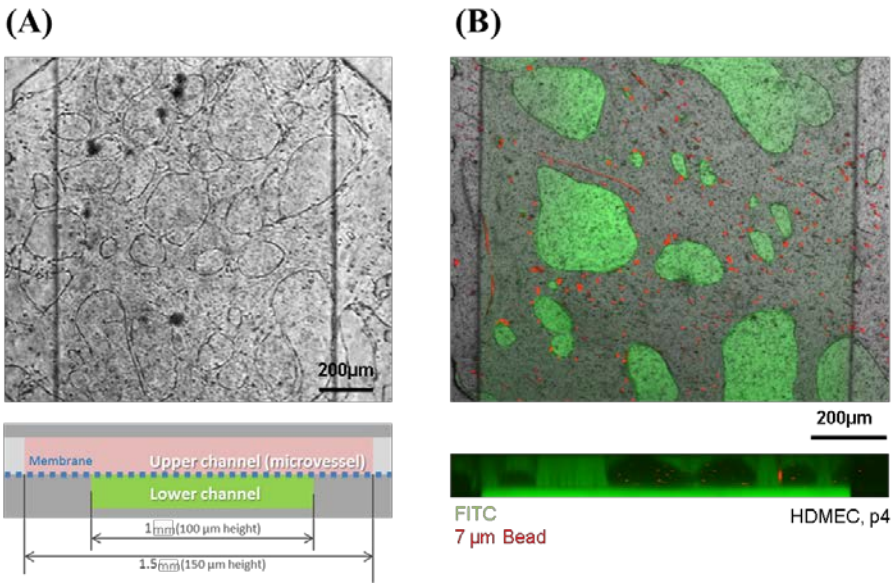


**Figure 2.4** Formation of perfusable microvessel. (A) Bright field image of the established in vitro microvessel. Micropost arrays provide the stable interaction between ECs and LFs resulting assembly of perfusable microvessel. (B) 7 μm microbeads (RFP) are injected in the interior of the microvessel while FITC-dye is accessed through lower channel.

### 2.3.2 FITC absolve and intensity difference

After confirming the formation of microvessel, next we have confirmed chemical transportation through porous membrane. We have selected the toxic chemical with SDS. SDS is widely used to test the toxicity. Before treating microvessel with SDS, first we tested with FITC dye because they have similar molecular weight 288 Dalton. After the microvessel is assembled, we injected FITC dye in lower channel. Right after the injection, 0 minute, we were able to notice the difference between inner and exterior of the microvessel (Figure 2.5). Exterior microvessel is highlighted with FITC fluorescent molecule while the inner microvessel is dark. FITC molecule cannot penetrate through the microvessel. 10 minutes after the injection, we were able to observe the microvessel absolving the FITC molecule from outside of the cell body. Whether or not the molecules have been washed out with the inner flow, inner lumen maintained dark while outer lumen seems to fade as time goes by. At the same time, the FITC molecule is absolved with microvessel wall. This experiment, we were able to confirm that the molecule size with 288 Da can diffuse from lower channel and transported to microvessel wall. We can expect SDS molecule can physic similar with this performance.

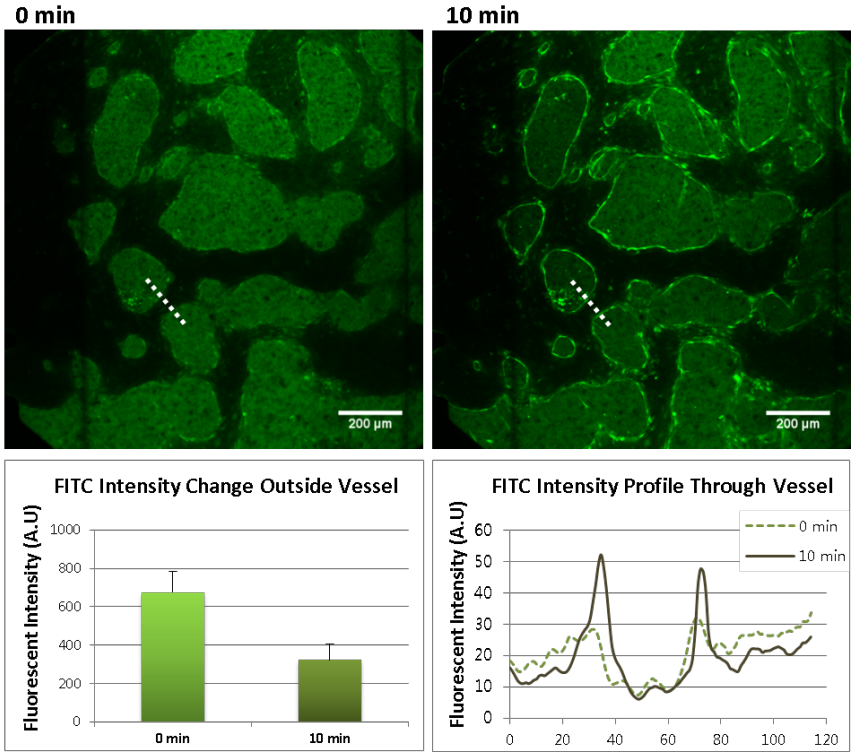


**Figure 2.5** Visualizing the exposure of chemical compound to microvessel with FITC dye (332 Da) (a) FITC dye is injected through lower channel and observed with confocal microscope, 0 min. Bright green indicate the exterior side of the microvessel while dark area is the interior side of the microvessel. After 10 min, FITC molecule is uniformly absorbed by EC cells representing molecule accessibility to microvessel through porous membrane. (b) FITC intensity change is measured by the time. FITC intensity seem to decrease along the time in exterior part while the microvessel wall have the opposite value. Also, interior part of the microvessel have no significant change meaning that the microvessel is well functioning as physical barrier resulting fluidic isolation.

### 2.3.3 Effect of 1% SDS

To test the microvessel behavior, we need to get rid of lung fibroblast as they might influence the microvessel behavior according to chemical. Therefore we used hydrogel-loop which is convenient to couple and decouple with the device. Here, we have assembled microvessel and after 7 days in vitro, we have removed hydrogel-loop capturing LFs. Stabilized microvessel can maintain their blood vessel formation for few days without the presence of LFs. Then we have mixed SDS 1% concentration, did live cell image to capture the deformation of the microvessel. We were able to see the damage in vessel wall just 30 seconds after (Figure 2.6). After 4 min later the exposure, we have fixed and immunostained the nuclei. Then, the area outside the chemical range, clear nuclei were detected while the exposed region, most of the nuclei has been damaged which means the toxicity lead to cell death (Figure 2.7).

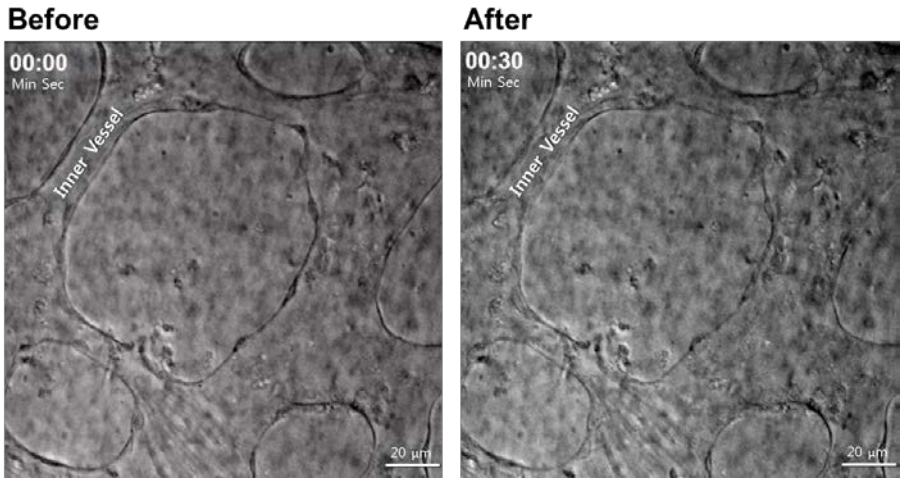


**Figure 2.6** Before chemical treatment, vessel is in healthy condition. After 30 seconds exposed to 1% SDS, damage of vessel wall is clearly observed.

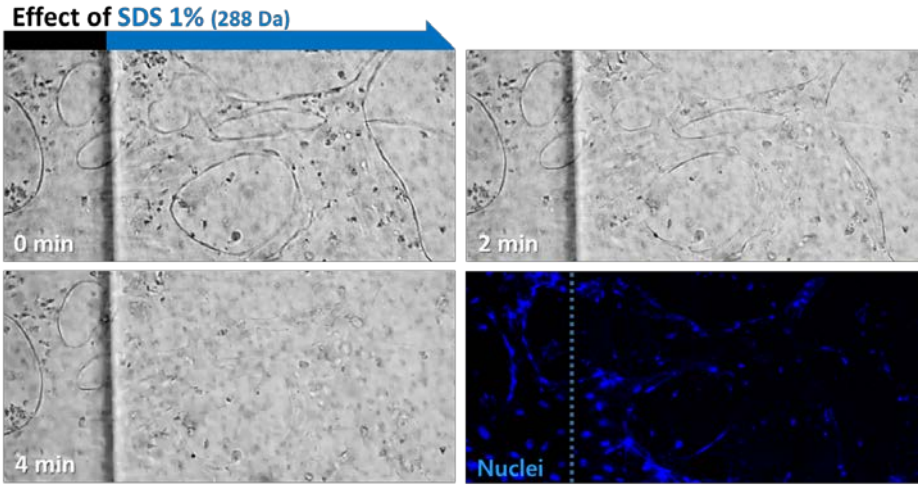


**Figure 2.7** Real-time observation of the effect of 1% Sodium dodecyl sulfate (SDS) to microvessel. We have tested our platform with 1% SDS solution to observe the microvessel morphology in real-time. Nuclei were stained to visualize the cell damage and we could notice that unexposed part is relatively viable

### 2.3.4 Effect of SDS according to concentration

To identify the device have potential to demonstrate the alternative chemical testing model, we have tested the microvessel with several concentration of SDS solution. We have diluted SDS in 0.1% v/v, 1% v/v and compared with control. To visualize the effect of the solution, FITC dye is mixed together. We expect the dye might penetrate through the microvessel if the vessel wall gets permeable enough according to the toxic solution. We have set up the experiment by holding device inside the confocal microscope stage. Tubes were connected and syringes were prepared filled with each solution. The images were captured with 2.5 seconds interval for 8 minutes. First we have tested with control, 0% SDS (Figure 2.8 A). Right after the chemical is injected, we were able to see the external region of the microvessel is glowing because of the FITC diluted in the solution. The inner region of the microvessel is dark because FITC cannot penetrate through the heathy vessel. We have maintained the condition longer than 8 minutes and inner vessel stayed clear which means the solution hardly affects the vessel wall. In Figure 2.8 B, we have drawn a line crossing inner and external vessels and arranged in a row. Each line in horizontal direction indicates the vessel condition at certain time and vertical direction indicates the time interval, 2.5 seconds per pixel. In control, we were able to find out FITC do not invade into inner vessel as time goes by. However, 0.1% SDS showed different result compared to control. The solution started to

damage vessel wall gradually. Longer exposure to solution make vessel wall permeable and allowed FITC to pass through. FITC start to appear at 1 minute and after 3 minutes, the dye spread most of the inner vessel area. 1% SDS gave more severe damage to vessel wall from the beginning. Vessel disappeared not longer than a minute and measuring time seemed meaningless.

By measuring the FITC intensity of the inner vessel we were able to draw intensity difference graph according to time (Figure 2.9). Here, we have selected the maximum intensity of each case as a complete damage. And we establish 40% of maximum intensity, as a standard intensity value point to specify the effect of chemical. From the graph, 0% SDS showed no increase of intensity profile. Even it relatively decreased while the external FITC value increase by the time. 0.1% SDS showed gradual increases and at 40s reached 40% of maximum intensity. 1% SDS showed steep incline according to time and reached 40% maximum intensity at 17.5 seconds.

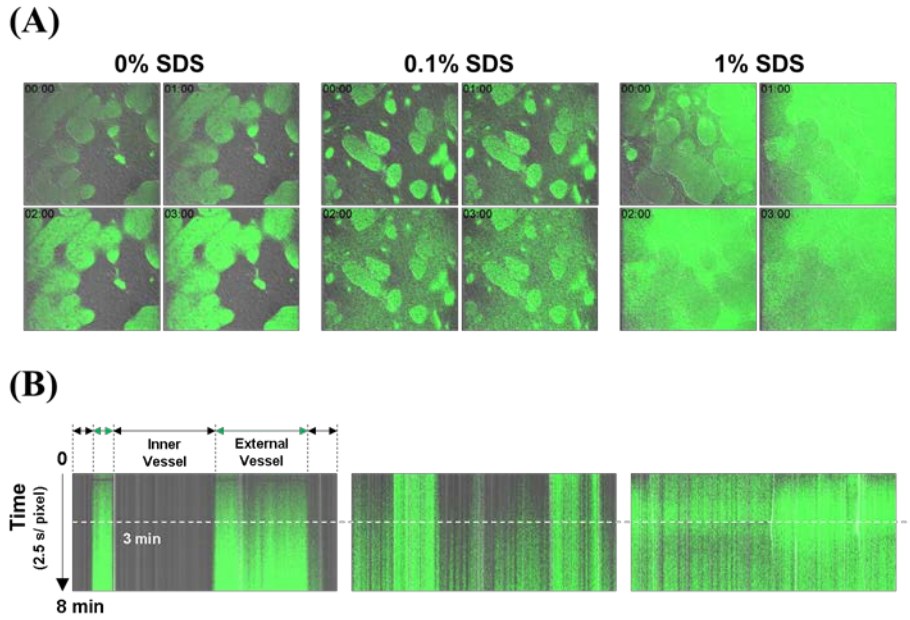


**Figure 2.8** Distinguishable result among compounds. (A) The platform is tested with 0%, 0.1% and 1% SDS. (B) Images are captured at intervals of 2.5 seconds. Each horizontal line pixel represent the time interval, 2.5 seconds. We can observe no change in 0%, starting to leak at 1 minute exposure to 0.1% SDS and immediate leak to 1% SDS.

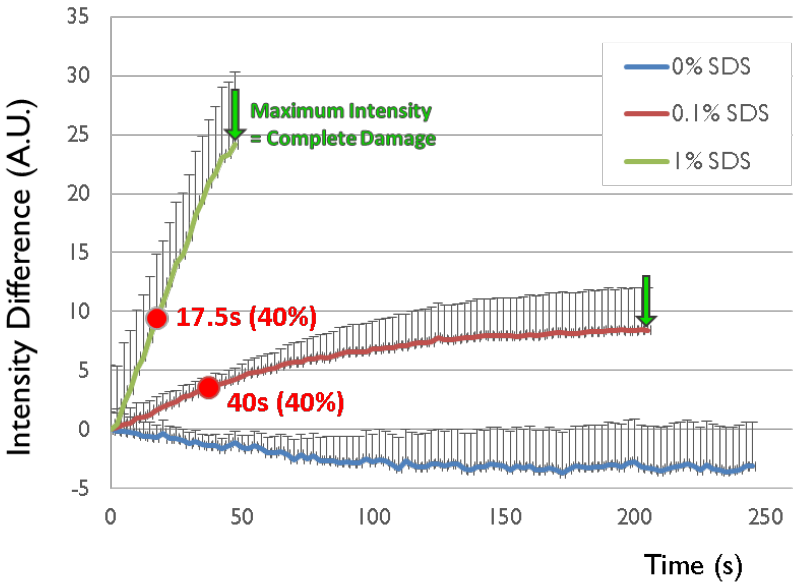


**Figure 2.9** Intensity difference graph according to time is measured from the data 0%, 0.1% and 1% SDS solution to healthy microvessel. 40% of maximum intensity is selected as standard intensity value point to distinguish time point among reagents.

## 2.4 Conclusion

Here in this chapter, we have demonstrated methods to fabricated double layered microfluidic chip with porous membrane in between. Using the device, we were able to successfully assemble vascular network by culturing HDMEC in three dimensional space supported with fibrin gel. LFs are trapped in a hydrogel loop which can be inserted and extracted freely within the reservoir. When LFs are inserted in the device, they can secrete growth factors for HDMECs to differentiate and assemble into blood vessel. After the vessel is formed, hydrogel loop containing LFs can be removed. As the experiment purpose is to observe the behavior of microvessel itself, it is novel idea to remove fibroblast from the device after the culture. Detail information about hydrogel loop experiment is descripted in chapter 4.

After the microvessel is formed, we have introduced SDS solution diluted in several concentrations. When healthy blood vessel is exposed to the 1% SDS solution, severe damage of the vessel wall is observed in a seconds. After 30 seconds, we were able to see microvessel fully damaged and falling down. Lowering the SDS within the solution has decreased the vessel damage according to time however, SDS solution itself is not fluorescent so it is difficult to measure quantitative results. Therefore we have selected mixing with FITC solution as their molecular weight is way similar, 288 Da. After mixing with FITC solution, we were able to measure the chemical penetrate over a damaged

vessel wall. Even when samples were not able to distinguish the damage with bright field image, fluorescent intensity can be measured. In regard to gradual damage, fluorescent intensity value can be measured by time and we have drawn out graph with 0%, 0.1% and 1% of SDS solution. Maximum intensity is where FITC intensity value become equal between inner and exterior side of the vessel. Before damage is observed with bright field image and can be detected with fluorescent value, we selected as standard value point, 40% of maximum intensity. There, with 0.1% SDS, it took 40 seconds to reach 40% of maximum intensity while 1% SDS took 17.5 seconds. These data shows discriminate results between samples.

Here we have presented *in vitro* irritancy test chip based on observing dysfunction of microvessel. We have success on establishing perfusable and accessible microvessel. With our designed device even low amount of fluorescent molecule can be detected and it have potential to be tested with more types of chemical which is hardly comparable with other assays. Irritancy of chemical ingredients in cosmetic products can be stringently tested with the device. The platform can provide discernment result among chemical compound and its concentration.

# 3 Platform #2 : “Open top” Two-layered Micropore Device to form Capillary Bed in vitro

## 3.1 Introduction

### 3.1.1 Embryology; the spatial relevance among cells

In order to fully develop the in vitro culture condition close to in vivo, we need to consider not only the cell types but also the spatial relevance among them. According to embryology, each body systems develop following their three primary germ layers in the early stage of embryo; ectoderm, mesoderm and endoderm. Ectoderm is the most exterior layer and differentiates to form the nervous system, hair, teeth and skin. Mesoderm develops muscle, bone and circulatory systems like blood and lymphatic vessels. Endoderm forms into the interior linings of two tubes in the body, the digestive and respiratory tubes. From the literature, we were able to find out that the blood vessel system lies in mesoderm layers in order to supply sufficient gas and nutrients efficiently [35]. Intimate contact and close interactions always occur among tissues and organs to maintain their functions in our body. Therefore, to provide similar in vitro co-culture niche for cells to express their native character, spatial term should be considered not only sufficient nutrient supply.

### 3.1.2 Tissue engineering and blood vessel

Tissue engineering covers cell biology, engineering, biochemical and physicochemical to improve or replace biological functions of tissues and organs in human body [36, 37]. Engineered tissues eventually transplanted fully or partially with disordering organs in patients. Therefore, to cultivate tissues or organs in vitro, it is important to select good cells and develop bioactive matrix which can cue cells to differentiate and assembled into functional tissue in three dimensional space [38, 39]. For transplanted tissues to be well grafted and fused with original tissue, it is important for them to induce fast vascularization as they need sufficient perfusion of nutrients. For example, patient with severe skin injuries from burn or diabetes will need engineered skin which can cover large area. When it is grafted on patients injured area, it is important for them to induce blood vessel fast as they need to be supplied with nutrients [40]. Otherwise, they might not perform well with surrounding tissues and lead to death of tissues. There are literatures which have verified pre-vascularized tissue can merge with original wound area faster than the one without vessel [31, 41]. Therefore, in the field of tissue engineering, establishing methods to cultivate vasculature with tissue is a big issue [42].

### 3.1.3 Blood vessel formation in microfluidic device

From approaches to establish vascular culture in tissue engineering, microfluidics is used to figurate the culture condition of endothelial cells and three dimensional hydrogels. However, as microfluidics can handle more precise control of micro environment compared to macroscopic tissue culture, naturally assembled blood vessels were able to assemble in microfluidic channels. Recent researches introduce novel methods to generate perfusable and functional microvessel in vitro. S. Takeuchi group suggested methods to make threads of hollow hydrogel with endothelial cell mixed [43]. There endothelial cell were able to make junctions each other to make vessel barrier. Later this experiment developed with tubing and success to perfuse and co-culture with other cells. N. Jeon group have engineered and designed to trap hydrogel in three dimensional structure in microfluidic device. By co-culturing endothelial cell and fibroblast within the microfluidic channels, they were able to establish naturally self-assembled perfusable microvessel [22, 44]. The application models and further experiments introduce co-culture with other cells such as smooth muscle cell, cancer and bone [45-48]. Also, small vascularized tissue models are introduced. T. Okano group suggested cell sheet method to culture layers of muscle cells filed up over perfused hydrogel matrix with endothelial cell attached [49]. Even though there are a lot of method introduced to co-culture cells and blood vessels in microfluidic device, there

still needs of findings in novel method to establish multiscale co-culture. It is excellent as it is to find cell-to-cell responses between vessels, however eventually the system needs to be scaled up for use in further possible researches and application models.

### 3.1.4 Aim of the device

Here in this chapter, we introduce our designed platform which provides co-culturing of vascular network and large sized cell spheroid. The device is spatially designed to culture cells in horizontal and vertical direction, which we expect that most of the three-dimensional culture condition can be demonstrated in the device. As similar with platform #1, it is also double layered however, the membrane part is monolithically fabricated by suggested unique method in this chapter. The lower part of the device is where the vasculature network is cultured and endothelial cells and fibroblasts are cultured in parallel channels. The important structured part is arrays of 200 μm sized micro pores in the middle of lower channel which connects upper and lower region. Upper, there is 6 mm open top reservoir which supports large sized cell spheroid. Therefore, large cell spheroid can be cultured on top of assembled blood vessel network with conformal contact according to micro pore. Here in this paper, we have cultivated microvessel longer than any

published data so far. Also, by connecting vascular networks, we were able to introduce fluid not only inner lumen but also exterior side of microvessel. By spatially separating the upper and lower channels with porous membrane, we were able to selectively flow different media within the channels. In this way, microvessel can experience different types of media supply at inner-and external side of the blood vessel barrier, which is usual condition for blood vessels in vivo. This condition realized in vitro is meaningful because selecting media is very important element to co-culture two types of different cells in one system. Finally we placed pre-cultured cancer spheroid on top of the pre-assembled blood vessel and observed microvessel behavior affected by cancer spheroid. Our development enables to overcome the difficulties experienced so far with existing devices and offers opportunity to design various experimental concepts in the field of microfluidic bioengineering.

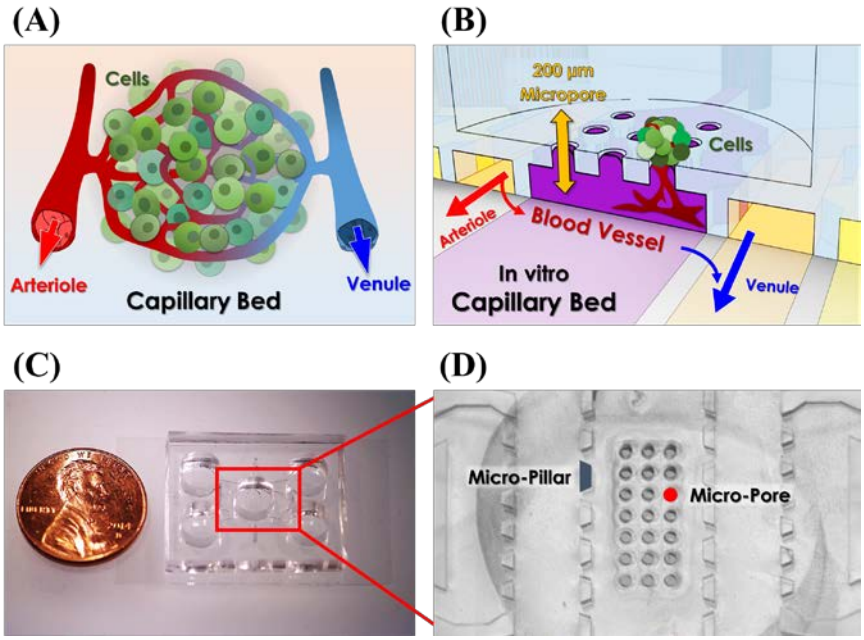


**Figure 3.1** Scheme of capillary bed and "open-top" microfluidic device. (A) Capillary bed is complex of dense microvessel and tissue. Nutrients are supplied to tissues while blood flows through microvessel, from arteriole to venule. (B) The device features similar structure with capillary bed. When blood vessel is assembled in the channel, media can flow from one channel to the other. By culturing cell spheroid in the reservoir, cells can experience close contact through micropore, which can enhance cell-to-cell interaction. (C) The device size can be estimated by comparing with penny. (D) Channel design. Fibrin gels are captured within micropillar walls and cells are cultured in 3D environment. Arrays of micro pores are located in the middle channel connecting upper and lower channels.

## 3.2 Material and Methods

### 3.2.1 Photolithography

In order to embed monolithic micro pore membrane in between upper and lower channels, several steps are followed (Figure 3.2). Pre-mold with reverse image of the device is firstly needed to begin the steps. To proceed photolithography pre-mold, two individual film photo-mask sets are drawn with commercial CAD program (AutoCAD, DE). Masks are overlapped to fabricate two layered wafer mold. First, wafer (Unisil, KR) is cleaned with plasma etcher (FEMTO Science, KR) and first layer on a clean wafer is spin-coated with SU-8 100 (Microchem, US) in 75 μm height for the micro posts (3000 rpm, 30 sec). Wafer is then soft-baked on a hot plate, 10 minute on 65°C and 45 minutes on 95°C continuously. Printed film photo mask (Hanalltech, KR) is then tightly contact to the surface of the wafer. UV radiation with 365 nm wavelength is exposed for the next step using conventional 500 W mercury lamp (Osram, DE) for 40 seconds (20 mW/cm$^2$, Seoungwoo MST, KR). After the exposure, wafer is post-baked on a 95°C hotplate for 10 minutes. Remaining photoresists are developed with thinner (AZ1500, KR) and designed patterns are obtained on the wafer. Second layer, additional 100 μm height is spin-coated with SU-8 100 (1250 rpm, 30 sec).Wafer is soft-baked on a hot plate for 20 minutes on 65°C and 90 minutes on 95°C. Film photo mask is precisely aligned over the first layer and tightly contacted for exposure. Expose UV radiation for 40 seconds to get a

pattern. Wafer is post-baked on a hotplate for 5 minutes and remaining photoresists are developed.

PDMS (Polydimethylsiloxane, Sylgard A/B, Dowcorning, US) is used to replicate the fabricated molds. Sylgard A/B is the commercial product from Dowcorning and prepared with elastomer base and curing agent. They are uniformly mixed in 10:1 ratio and degassed in a vacuum pump. Degassed mixture were then poured on a silicon wafer molds and baked on a 95°C hotplate. After PDMS is polymerized, it is detached on a wafer and trimmed in a right size to use.

### 3.2.2 Device design and fabrication

We fabricated the microfluidic chip using combined method of standard photolithography and soft-lithography techniques (Figure 3.2). By the standard two-layered photolithography technique, we developed positive shape of the platform on the wafer surface. We replicated the negative shape of the platform, called as pre-mold, with PDMS, and plasma-bonded on the slide glass. Anti-adhesive solution was coated in between the PDMS and slide glass. Then, PDMS precursor was filled in the gap without air bubbles, and solidified. Pre-mold with the bottom layer of the platform was detached from the glass by force. Blank PDMS piece with a punching-hole was plasma-bonded on the top of pre-

mold complex, which will form top layer of the platform. Open-top device and pre-mold could be easily separated. Trans-membrane is also embedded within the device, since the post, which was previously on the pre-mold, was conformal contact to the slide glass. After oxygen plasma treatment on both glass coverslip and device, microfluidic platform was stored in dry oven to regain hydrophobicity.

### 3.2.3 Cell culture

Human dermal micro-vascular endothelial cell, HDMECs (Lonza, Basel, Switzerland) were cultured in the endothCelial growth medium (EGM-2 MV; Lonza), and cells between passages 4 to 5 were used. Primary human lung fibroblasts (Lonza) were cultured in fibroblast growth medium (FGM-2; Lonza), and passages 6 to 10 were used for the experiment. To harvest the cells, they were rinsed with phosphate buffered saline (PBS) and treated with 0.25% trypsin–EDTA (Gibco, Carlsbad, CA). After 2 min, M199 (Lonza) containing 10% fetal bovine serum was added to neutralize the effect of the enzyme. Detached cells were collected and centrifuged for 2 min in 1100 rpm, and diluted in EGM-2 to reach a certain cell number in the suspension.

### 3.2.4 Culturing U87MG spheroid

Human glioblastoma cells, U87MG (ATCC, Virginia) were cultured in DMEM (Hyclone) supplemented with 10% FBS, penicillin (100 U/ml) and streptomycin (100 U/ml). Cells are prepared in 0.15 mil/ml concentration and hanged upside down with each 20 μl on a cell culture dish. To prevent small amount of droplets from evaporation, cell culture dish is filled with sterile water. Cells are maintained in a humidified incubator at 37˚C and 5% $CO_2$. After 2 more days in culture, cancer spheroid sized 300~ 500 μm is formed.

### 3.2.5 Cell loading

HDMEC and LF is cultured in lower part of the device and U87MG spheroid is cultured in upper part of the device (Figure 3.3 A). To assemble vascular network in the device and co-culture with spheroid, first each fibrin and HDMEC and LF mixture is prepared (Figure 3.3 B). HDMEC is injected in middle channel and LF is injected in side channels and fresh media is supplied through all five reservoirs. Cells are maintained in a humidified incubator at 37˚C and 5% $CO_2$ and media is changed in every two days. After 3 days, cancer spheroid is placed over the vasculature channel. Next, for cancer spheroid angiogenesis culture, first empty fibrin gel is loaded in middle channel and LF is loaded in one side of channel. Next, HDMECs were loaded in to reservoir

and attached to hydrogel wall. Then cancer spheroid is placed on top of the empty gel channel and maintained in a humidified incubator at 37˚C and 5% $CO_2$ and media is changed in every two days.

### 3.2.6 Immunostaining

To configure the physiological relevance of the blood vessel, samples were fixed with 4% paraformaldehyde. They were permeabilized with 0.15% Triton X-100 for 15 min and treated with PBS solution containing 3% bovine serum albumin (BSA; Sigma-Aldrich, St. Louis, MO). To visualize the lumens of the blood vessel, green fluorescent protein–conjugated CD31 (Biolegend) was used with a ratio of 1:250, and Hoechst 33342 (1:1000) for the nucleus. RFP-conjugated phalloidin (1:100) is used to visualize U87MG. Fluorescent images of the capillary were taken with the confocal microscope with every 3 μm height. The stacked images were deconvoluted into 3D volume using IMARIS. For live cell imaging, images were taken with 2.5 second interval.

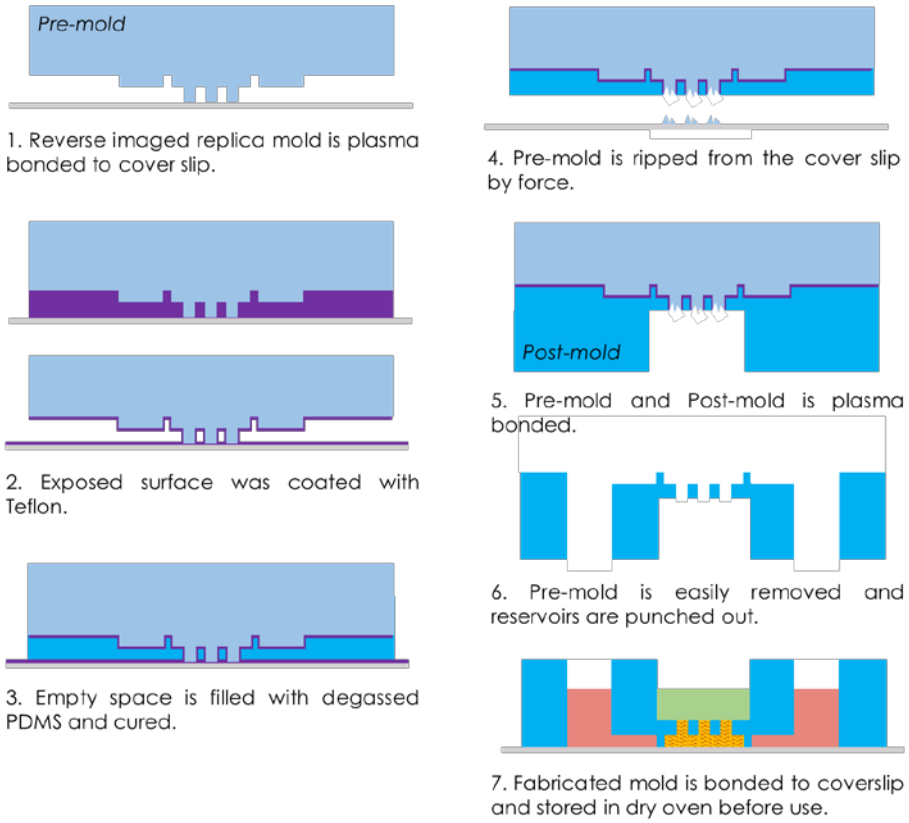


**Figure 3.2** Fabrication Procedures of micro-pore embedded microfluidics. We have made inversed PDMS pre-mold to have both micropillar and micropore in a thin membrane. By coating with Teflon, we were able to make boundaries and prevent same materials merge together. As pre-mold is featuring inversed topology, micropost become micropore and pores become pillars. Post-mold with reservoir removed is bonded and the device is ready for the next step

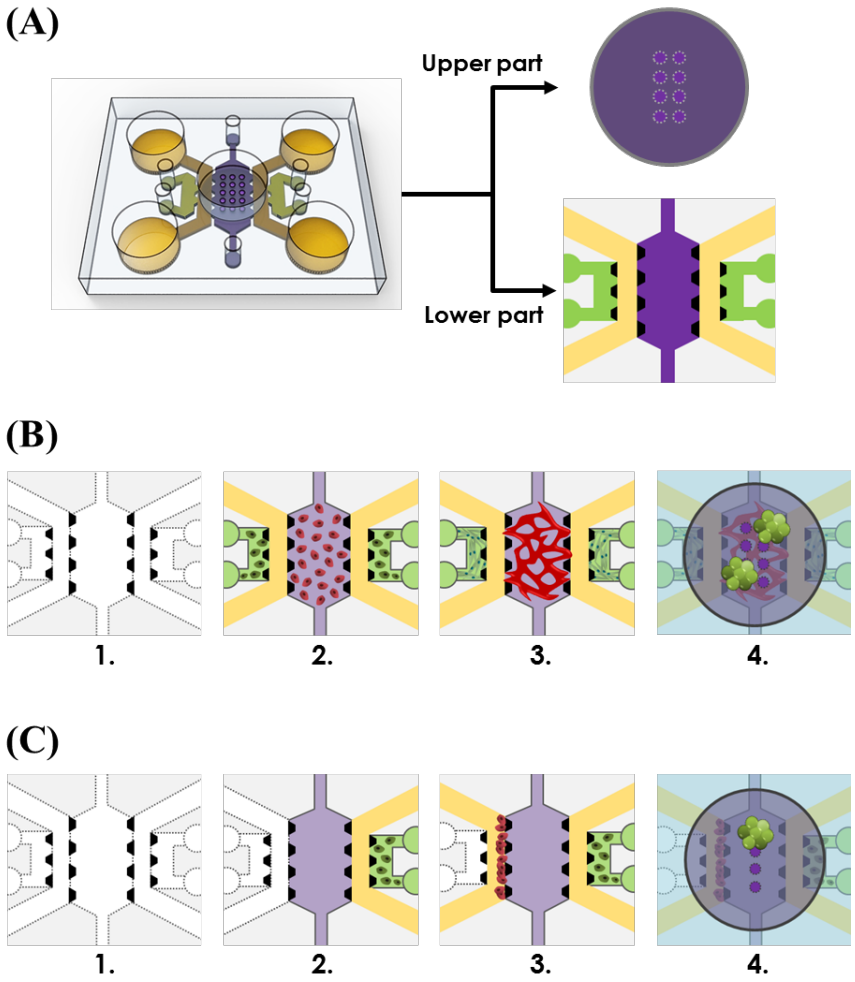


**Figure 3.3** (A) Design of upper and lower channel of the Platform #2. (B) Method steps to co-culture vascular network and cancer spheroid. (C) Method steps to induce angiogenesis co-cultured with cancer spheroid.

## 3.3 Results and Discussion

### 3.3.1 Micro vessel formation in the Open top microfluidic device

We have cultured HDMEC in the middle channel and LFs in the each side channels both mixed with fibrin gel. HDMEC channel is 2 mm in width and 100 μm in height. Since the channel width is longer than original microvessel device [22], we have supplied additional fresh media through micro pore on top of the channel. In 3 days in vitro, HDMECs start to elongate and make connection with nearby cells (Figure 3.4 A). In 5 DIV, vacuoles grow within the cells and linked together to make hollow tube and random microvessel networks are assembled. Microvessel have openings at hydrogel boundary between micro posts. Therefore, media can flow from one side to the other, which makes microvessel perfusable (Figure 3.4 B). We have visualized perfusability of microvessel by dropping FITC dye in reservoir while cells are still alive. Hollow lumens are filled with green fluorescent dye in every corner of the microvessel and we can see microvessel network clearly. After few minutes, FITC molecules penetrate through blood vessel barrier and diffuse in surrounding gels. By immuno-staining HDMEC with CD31 endothelial cell marker, microvessel connection and size of the lumens were imaged with confocal microscope.

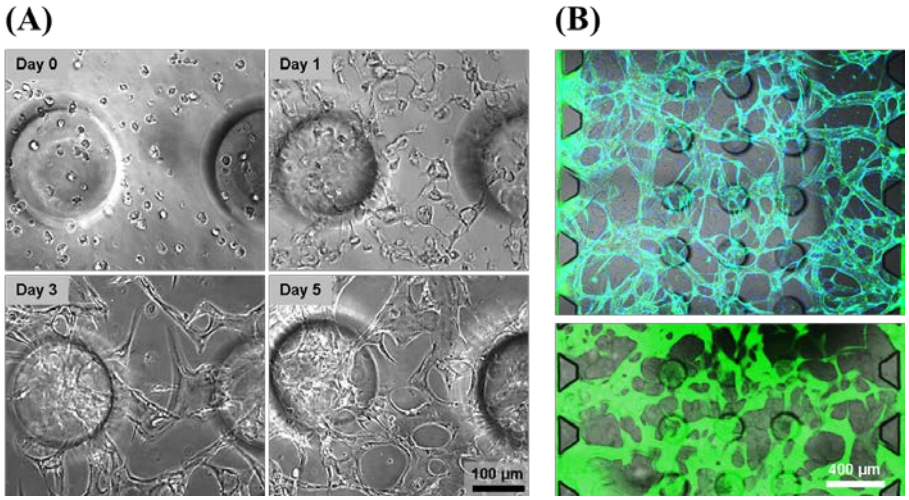


**Figure 3.4** (A) Formation of microvessel in an open-top micropore device. We have observed endothelial cells assembling each other day by day. (B) To visualize the microvessel formation, cells are stained with CD31 and nuclei. FITC dye can flow inner lumen while microvessel is alive.

### 3.3.2 MIcro vessel formation according to channel width

Open-top microchannel can enhance the media supply throughout the channel and improve culture condition. Therefore, cells can live in microchannel with longer channel width. Here, we have compared cell ability to perform as microvessel in micropore channel and control channel. We have figured microchannel in several widths, 2 mm, 3mm and 5 mm. Only the difference with control is the existence of micropore. In 2 mm, there are 3 columns of pores and 5 for 3 and 5 mm channels. Both cells showed elongated shape and network connection in some part of the channel. However, cells in micropore device showed thicker lumen diameter compared to control (Figure 3.5). In 2 mm device, microvessel in both devices have similar diameter of lumen in x-y plane. However, in z-direction, micropore device have thicker diameter compared to control. This showed to the other conditions too.

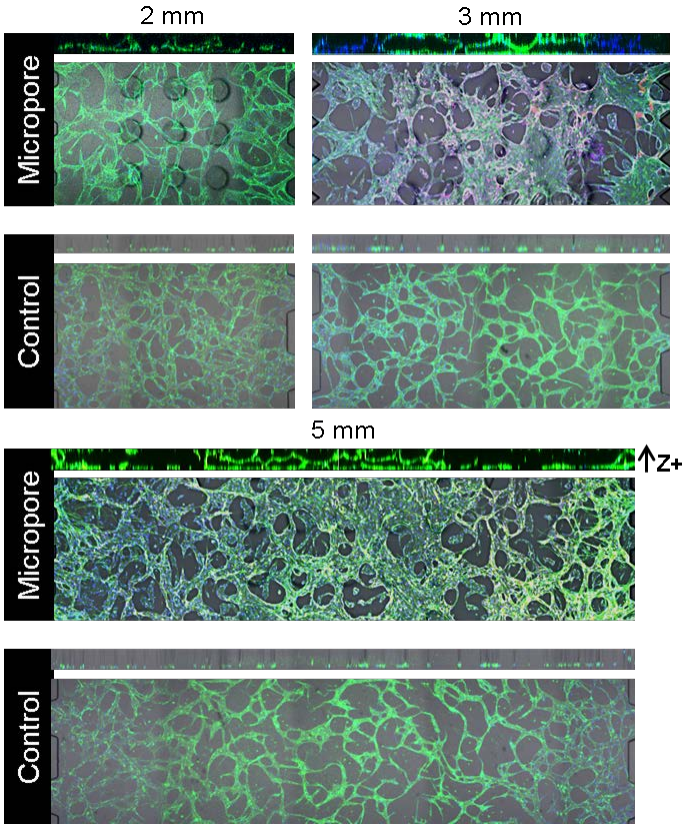


**Figure 3.5** Micropore device is compared with control. Fresh media can be delivered to center channel through micropore so culture condition ca be enhanced. Compared to control, we were able to observe that in the micropore channel, blood vessel can be linked well and have perfusable lumen. The control, even though cells are alive, we were not able to observe any lumens.

### 3.3.3 Selective Fluid Delivery to Intra- and Extra-Luminal Side of the Microvessel

One of the biggest advantage of the device is that it is possible to treat two types of media at the same time. Once the microvessel is formed inside the defined microchannel, the gaps between micro post arrays become the vessel opening. From this structure, media introduced to reservoir can travel through one channel to the other flowing through intra-luminal side of the microvessel. The media flowing inside the microvessel can be prohibited to diffuse out by blood vessel barrier since the cells are attached tightly each other. Also, the media dropped on top of micro pore channel can spread down to lower channel (Figure 3.6 A). To demonstrate the capability, we have used red-dextran and FITC dye. Intra-luminal side of the microvessel is filled with red dye, while FITC saturate the hydrogel. Reverse intensity signal is measured between two dyes following selected line. FITC did not observed in intra-luminal side while Dextran didn't appeared in extra-luminal side (Figure 3.6.B). This condition has maintained over 30 minutes (Figure 3.6 C). Only small amount of FITC has been spread in the hydrogel matrix. From this result, we can expect continuous experiment using appropriate medium combination.

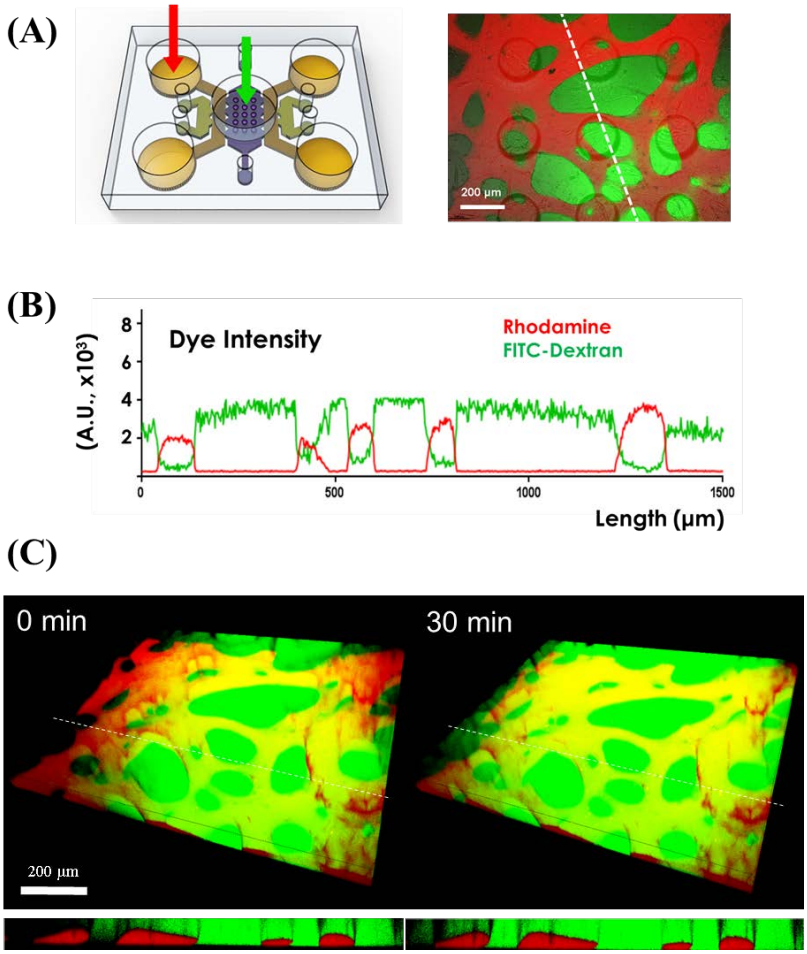


**Figure 3.6** (A) After blood vessels are fully developed in a micropore channel, we have flowed red dye through the outer reservoir and green dye through center reservoir. Red dye can flow inside the inner blood vessel and green dye can access exterior side of blood vessel. (B) The dye intensity graph clearly shows opposite peak where blood vessel wall stands. (C) This condition has maintained for 30 minutes.

Next, we have selected two types of medium to observe the microvessel behavior against combination sets of medium condition; EGM2-MV (EGM) and Epilife (EPI). Epilife with conditioned supplement is medium to culture keratinocyte cells from animal skin. As introduced in introduction part, keratinocyte and endothelial cells originate from different germ layers, which means they cannot share common medium. Likewise typical trouble shoot in co-culturing two or more types of cells, selecting appropriate medium is always an issue. In this experiment, we tested with four combination sets of two mediums and maintained for two days (Figure 3.7 A). After culturing perfusable microvessel, devices is washed with PBS and following medium combination is introduced in intra/extra side of microvessel; EGM/EGM, EGM/EPI, EPI/EGM and EPI/EPI (Figure 3.7 B). Same spot is imaged before and after two days and we have measured 10 microvessel for each sample to figure out the tendency in diameter difference (Figure 3.8). In the case of EGM/EGM, there were increase in microvessel diameter. EGM/EPI and EPI/EGM showed similar results. They showed slight increase or decrease but mainly they maintained their vessel thickness. However, when the medium combination is both used in EPI, there were shrank in microvessel. This result indicate microvessel can survive and maintain their morphology unless all of the medium is replaced with not favored condition.

(A)

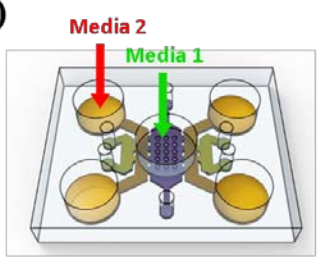


| | | |
|---|---|---|
| **Set 1** | Media 1 | EGM |
| | Media 2 | EGM |
| **Set 2** | Media 1 | Epilife |
| | Media 2 | EGM |
| **Set 3** | Media 1 | EGM |
| | Media 2 | Epilife |
| **Set 4** | Media 1 | Epilife |
| | Media 2 | Epilife |

(B)

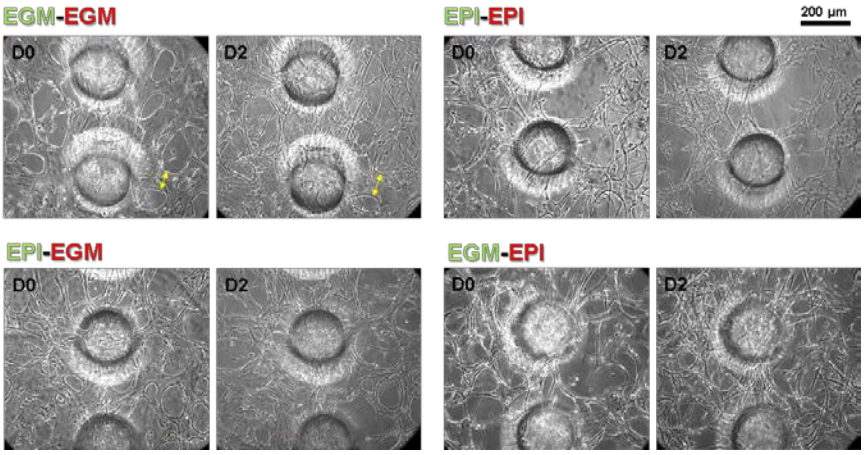


**Figure 3.7** (A) Four sets of experiment media combination is listed. (B) We have cultured microvessel in different media condition for two days. Yellow arrow in EGM-EGM sample indicate the difference in vessel diameter. Ten vessels are measured from each sample.

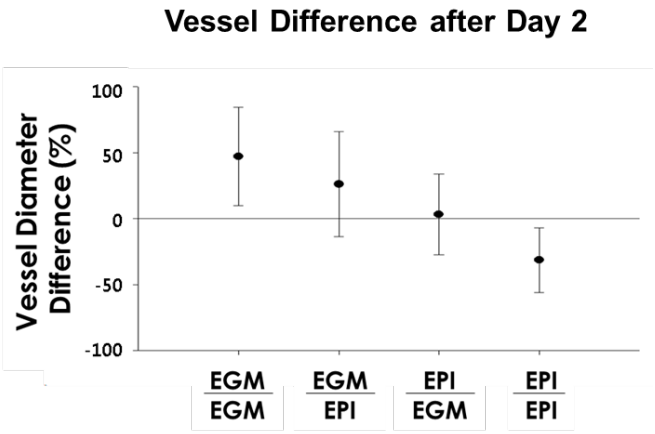


**Figure 3.8** We were able to experience difference in vessel diameter. With the original medium condition, vessel wall grew about 50% larger. When the medium is different in upper and lower channel, vessel experienced little growth or sustained. When we used the medium which is not for EC culture, vessel shrank or degraded.

The capacity of the device in selective fluid delivery, also can implement chemical irritancy test which is specified with platform #1. After culturing perfusable microvessel, we have visualized inner microvessel with rhodamin-dextran. Next, we have prepared 0.2% SDS solution mixed with FITC dye and dropped on top of the microvessel channel. Images were taken in 2 second interval (Figure 3.9). Intensity value graph is drawn according to white dashed line. At 0s, only Rhodamin is observed while chemical solution is not yet spread to microvessel. In 12s, FITC is observed surrounding the microvessel. As time flows, microvessel is gradually damaged by toxic solution and by 24s, rhodamin start to burst out to extra hydrogel. However, even though the solution interrupted the function of microvessel barrier, FITC solution overall showed increase in overall background intensity while it doesn't flow inside the lumen, which means there is constant flow in intra luminal side of microvessel.

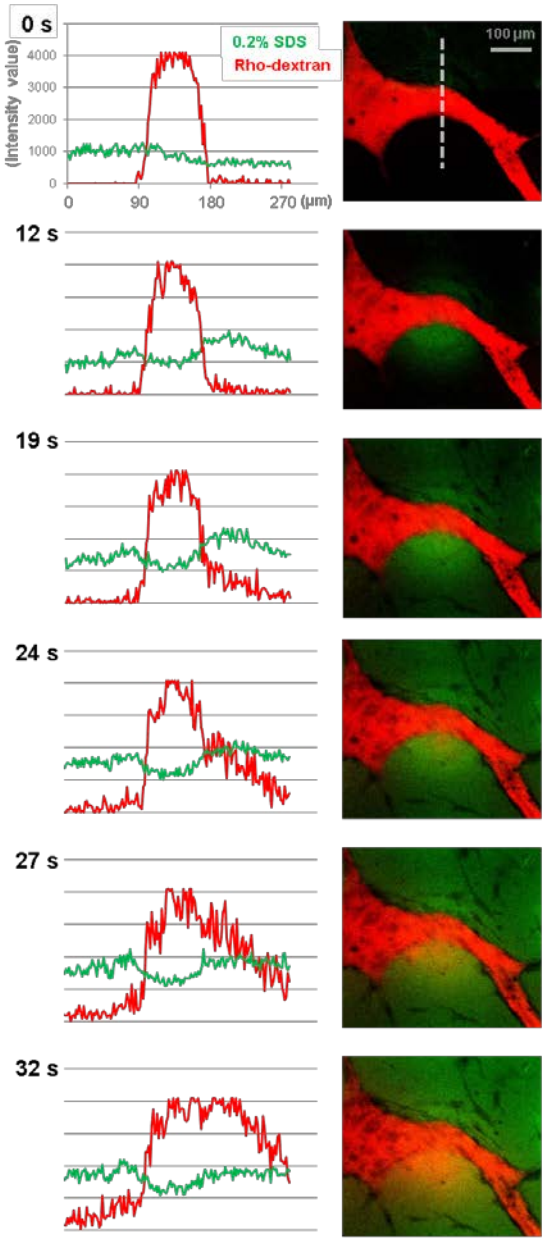


**Figure 3.9** Toxicity test can be performed with Platform #2 as well. Rhodamin-Dextran in filled inside the lumen. When SDS solution spread down through micro pore, vessel wall start to leak at time 24s.

### 3.3.4 Culturing cancer spheroid on top of the vascular network.

Last experiment performed with the device is co-culturing vascular network with cancer spheroid. As introduced previously, the device is designed to culture cells in spatially defined microchannel. Endothelial cells and fibroblasts are cultured in parallel channels in same plane to assemble perfusable microvessel. On top, vertical direction, cancer spheroid is loaded after vascular network is formed. Here, we used U87MG and cultured in spheroid by hanging drop method. According to scale bar, we can determine the size of the cancer spheroid. Usually their size differ from 250 to 500 μm. As they can grow larger than general microfluidic channel dimension (~ 150 μm) fabricated in photolithography method, it is difficult to squeeze them into microchannel. However, using the platform #2, we can simply drop the spheroid open top reservoir and fit them over the micro pores. By removing mediums in side four reservoirs and filling center open top reservoir, micro pores become sink according to hydrostatic pressure. Dropped spheroid can float and settle on top of the micro pore easily. After the spheroid lies on the pore, rest of media is supplied at side four reservoirs and cultured for additional 7 days. After 1 day, spheroid can adhere with the device and settle down firmly. We have demonstrated the size of the pore and dropped cancer spheroid. Larger pore, cancer spheroid can have large area contact with vascular network directly (Figure 3.10 A). From this experiment, we have demonstrated the capability of

the device. The size of the pore can be designed according to tissue used instead of cancer spheroid.

In the experiment, we used platform with 200 μm micro pore. We decided 200 μm pore is the appropriate size compared to the vessel opening, formed in between micro post arrays. The dimension of the gap area is 100 μm in horizontal and 100 μm in vertical. We decided the micro pore size in between the size of vessel opening and cancer spheroid. Also the average diameter of microvessel is around 50~150 μm formed in vascular network is considered. Cancer spheroid can surely affected the growth of microvessel. U87MG can secrete VEGF which can induce endothelial cells to form microvessel [50]. From several experiment performed in this paper, we have demonstrated the effect of cancer spheroid to microvessel. They can affect their growth in vessel thickness, number of branches and their orientation.

First, we observed conformal contact between cultured vascular network and cancer spheroid. Cancer spheroid is cultured on top of the microvessel for 5 days and stained with CD31-488 nm, phalloidin-594 nm and Hoechst-405 nm. CD31 is endothelial cell specific marker, which we can observe HDMEC only. The antibody is conjugated with GFP. We stained f-actin with phalloidin conjugated with RFP to observe cancer cells. As phalloidin can stain f-actin in both HDMEC and U87MG, to distinguish between two, cells emitting only RFP can be considered as U87MG while endothelial cells can emit both RFP and

GFP. As cancer spheroid can have conformal contact with microvessel area, they have as much chance to interrupt each other. Depth of the micro pore depend on the thickness of membrane. Here, we have configured the depth of the micro pore as 75 μm. As explained at material and method section, the pore can be either filled with media or hydrogel according to surface condition. In either condition, cells can travel along the pore surface and their distance is minimum 75 μm which can be considered spatially close situation.

We can visualize the difference between the vessel with and without cancer spheroid. The vessel right underneath the spheroid, many cancer cells have traveled down from upper open-top reservoir and surrounded the external region of the vessel (Figure 3.10 B). Also, from the cross-section image, cancer cells are closely attached to microvessel wall. This is important result because from previous co-culture experiments, they had lower probability compared to this experiment because they used dispersed single cells [46, 47]. Contrary, vessel wall and its surrounding is clear in the sample without cancer spheroid. Cells only expressing both signal can be detected along the vessel surface which informs the vessel is only composed with endothelial cells.

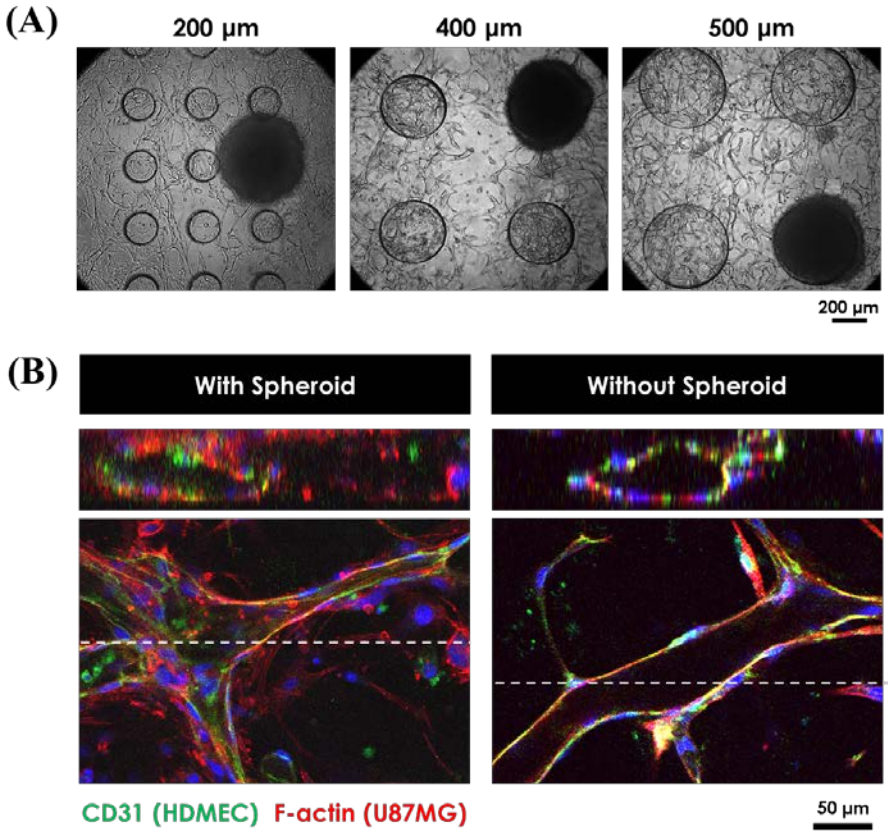


**Figure 3.10** (A) After blood vessels start to make vessels in a micropore channel, we have loaded cancer spheroid (U87MG) on top of the micropore. Cancer spheroid are about 400 ~ 500 μm large. The pores are designed in several sizes. (B) Immuno-stained micro vessel. We have observed cross-section of the blood vessel. Cancer cells migrated downwards to microvessel right under spheroid, and covered around the microvessel. Green is endothelial cell and red is F-actin which stains both cell. However, microvessel without spheroid have more clear vision and no other cells surrounding blood vessel.

### 3.3.5 Blood vessel recruitment

We have observed the difference in the growth of microvessel with and without cancer spheroid culture. As introduced in material and method, U87MG is known to secrete VEGF to induce blood vessel formation. So as to prove the fact, microvessel co-cultured with U87MG spheroid has been enhanced in growth. Before combining with cancer spheroid, we start with endothelial cell and fibroblasts to assemble microvessel in the channel. LFs also secrete a lot of VEGFs which is enough for ECs to differentiate. To insist the pure effect of cancer spheroid, we have compared with the presence of fibroblasts in the culture. Channel width of the micro pore area is 5 mm to distinguish the effect within the device. According to the width of the EC channel, total amount of ECs and hydrogel is decided. Also, the distance of ECs from center to LFs in side channel gets further. Therefore, transportation of growth factors secreted from LFs cannot reach ECs in the middle area. To overcome this issue, we can prepare EC and LF hydrogel mixture. Then the additional LFs mixed within ECs also can secrete factors and enhance culture condition. We have composed four sets of experiment. One set of HDMECs are mixed with LFs in the hydrogel, while the other set of HDMECs cultured alone. Then, cancer spheroid is placed on one of each sets. After culturing the cells for 5 days, we were able to compare the difference among four sets.

Firstly, microvessel mixed with LFs and have cancer spheroid on top of the

channel (+/+) have abundant vascular networks (Figure 3.11 A). However, when there is no cancer spheroid around (+/-), they have less thickness of microvessel. But LFs can help ECs to elongate and connect each other. If there is no LFs mixed with ECs, generally cells have failure in connectivity. Sample only with cancer spheroid (-/+) have better vascular formation compare to ECs with neither VEGF source cells (-/-). Further, in (-/+) sample, we were able to observe the difference in microvessel according to the distance from cancer spheroid. Microvessel near spheroid have thicker vessel diameter. From this experiment, we were able to understand the different outcome from the sets and observe the effect of LFs mixed with ECs. When LFs are spread uniformly within ECs in 1:20 ratio, they can enhance the connectivity of the endothelial cells. Similarly, cancer spheroid can also enhance the growth of endothelial cells by effecting the thickness of microvessel. As the two type of cells are well known as VEGF secreting cells, using both cells bring out the best results. We have measured the thickness of vessels and compared among each samples and plotted in graph. We have divided the vessel network area in nine and from each part we have selected ten vessels and measured total 90 vessels (Figure 3.11 B). The difference between samples comparing with and without LFs showed meaningful data. And the presence of cancer spheroid can affect the formation of the microvessel and bring out different results nevertheless there is an effect of LFs.

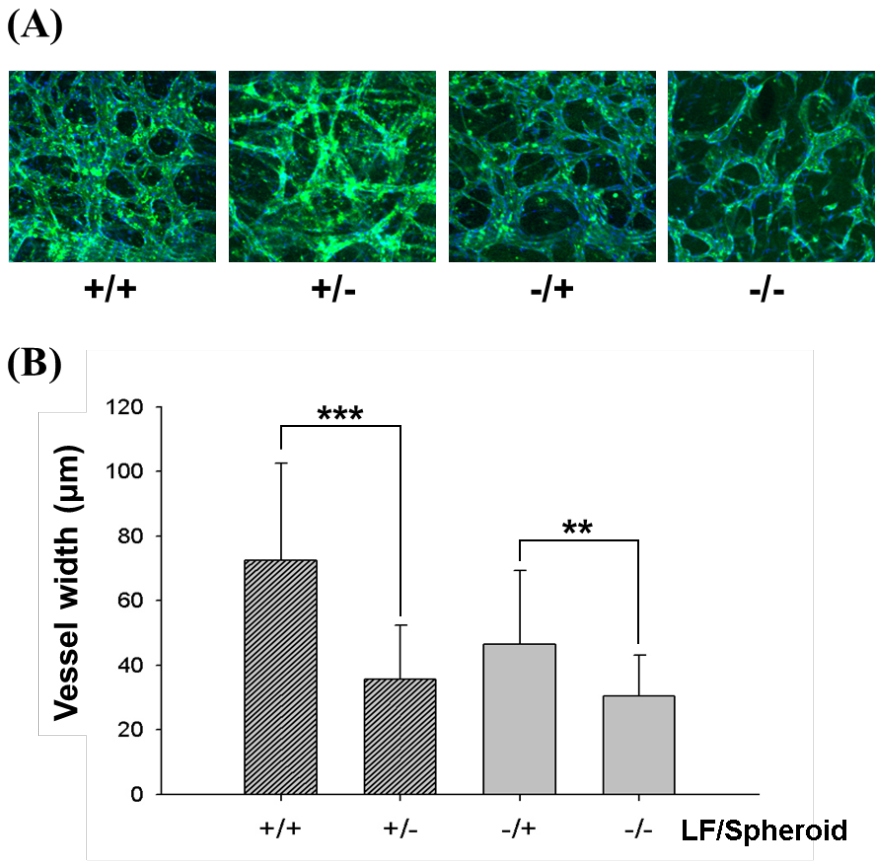


**Figure 3.11** (A) Four sets of cell combination (LF/Spheroid). First two images both have LFs mixed with vessel and only the first one is co-cultured with spheroid. Next two images are without LFs and third image is co-cultured with spheroid. (B) By comparing the vessel width, Spheroid can enhance the growth of vessel diameter. From the figure, LFs affected connectivity.

In the next experiment, we focused on the microvessel recruitment caused by cancer spheroid. Like the same, we used large area micro pore channel with 5 mm width to distinguish the effect of cancer spheroid to microvessel. If we use 2 mm width device in this experiment, whole microvessel area is affected by cancer spheroid and they appear same behavior whether they are there or not there directly underneath the cancer spheroid. In contrary, 5 mm width channel have large enough area to compare the local difference formation from the effect of cancer. After culturing ECs for 2 days in the device, we have randomly positioned the cancer spheroid and cultured additional 5 days together. Endothelial cells are immunostained with CD31 to observe only the microvessel. Then, we were able to observe that in the same device, there were different density of networks according to distance from cancer spheroid (Figure 3.12 A). Cancer cells showed their ability to guide endothelial cells towards them and enhance their growth. Expression of CD31 is detected bright near the cancer which means the dense network of microvessel. To figure out the vessel recruitment in this experiment, we decided to measure the intensity of fluorescent value of CD31 where the pores are located (Figure 3.12 B).

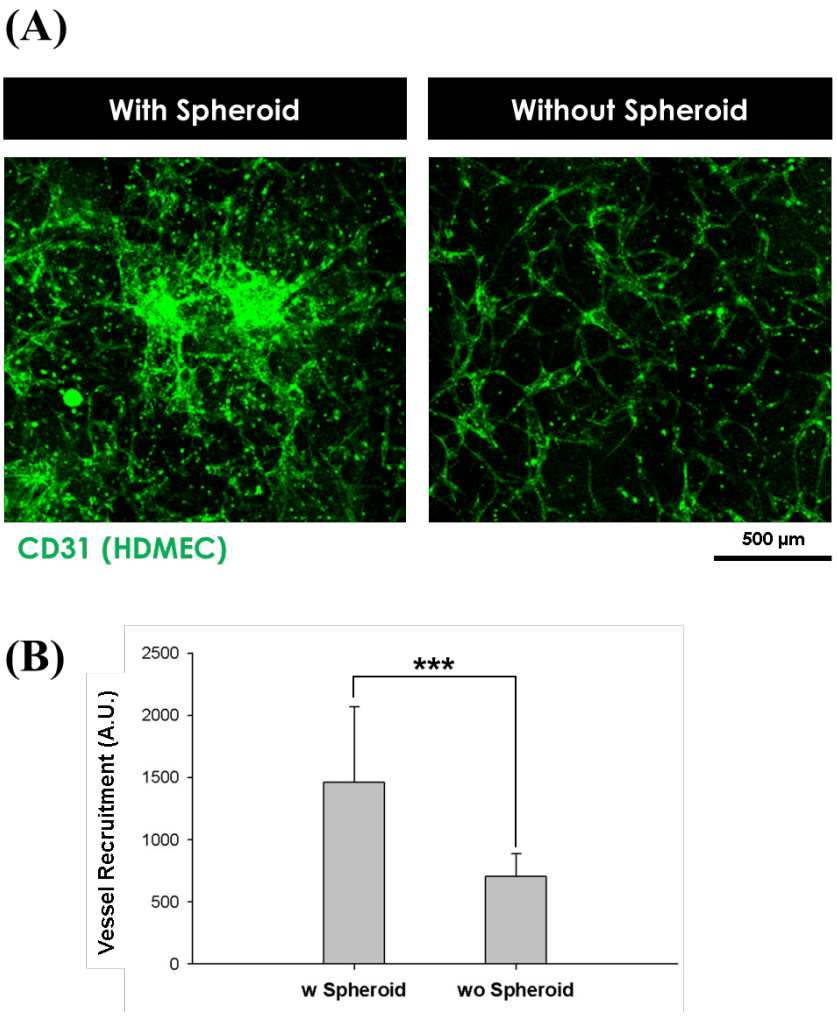


**Figure 3.12** (A) Vascular network with and without cancer spheroid showed difference in their growth. (B) We have measured intensity of CD31 where micro pores overlap. Micro pores around spheroid had higher intensity value compared to the pores far from spheroid.

In order to apply the cancer spheroid ability to recruit the microvessel, we further tested angiogenesis induced with cancer spheroid. Unlike experiment so far, we have placed HDMEC on the wall of empty fibrin gel (Figure 3.3 B). Detail experiment information is written in material and method part. Micro pore array is arranged in a line so it is easy to estimate the position of the spheroid. In Figure 3.13, endothelial cells stretched their sprout towards the cancer spheroid. From the experiment, we were able to well demonstrate the situation where the spheroid are locally positioned and secreting VEGFs. In this condition, ECs were able to freely grow and differentiate into microvessel following the conditions.

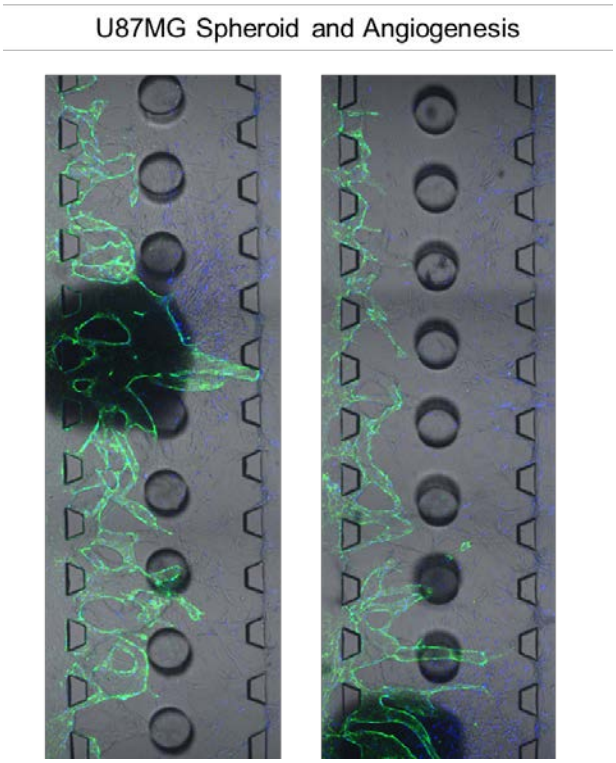


**Figure 3.13** HDMEC is attached on a hydrogel wall and angiogenesis is induced by LFs and U87MG spheroid. Faster growth of microvessel sprouts are observed near cancer spheroid.

### 3.3.6 Vertical angiogenesis towards cancer spheroid

"Open top" micro pore device is designed to co-culture cells not only in horizontal direction but also in vertical direction. Cells morphology and the mobility behavior can be detected in vertical z direction not only in x-y plane. The purpose of the device is to co-culture vascular networks and small sized tissue and observe their interaction and fusion. Until this experiment, we continuously detected the effect of cancer spheroid and proved their ability to recruit microvessel. Last outcome we were able to obtain is to figure out whether the microvessel can sprout towards the cancer spheroid placed above themselves. We have seen the cancer cells migrate downwards and surrounded the vessel. And we expected to observe the vessel can sprout into the U87MG spheroid. Unfortunately, against our expectation, we cannot perfectly witness the vessel formation inside the cancer spheroid as they are tightly attached to each other and have no extra space for microvessel to evade. Even though they cannot go through, they were able to reach and contact to spheroid as the micro pores can guide their path. While the vessel is alive and enable to maintain their barrier function, we introduced FITC dye and filled all the hollow lumens (Figure 3.14 position 2). Surprisingly, FITC dye is detected on top end of micro pore which means there exist functional vessel. Images snapped in z direction is reconstructed with IMARIS to visualize their distribution. Blue dotted line in cross-sectional x-z plane indicate where micro pore is defined and white arrow

directs the FITC filling in vessel lumen. These vessels are detected at micro pores lied underneath the cancer spheroid. To check the precise formation of vessel, we again fixed the sample and stained with CD31 (Figure 3.14 position 1). Like the same with position 2, vessel sprouts are detected clearly in vertical direction.

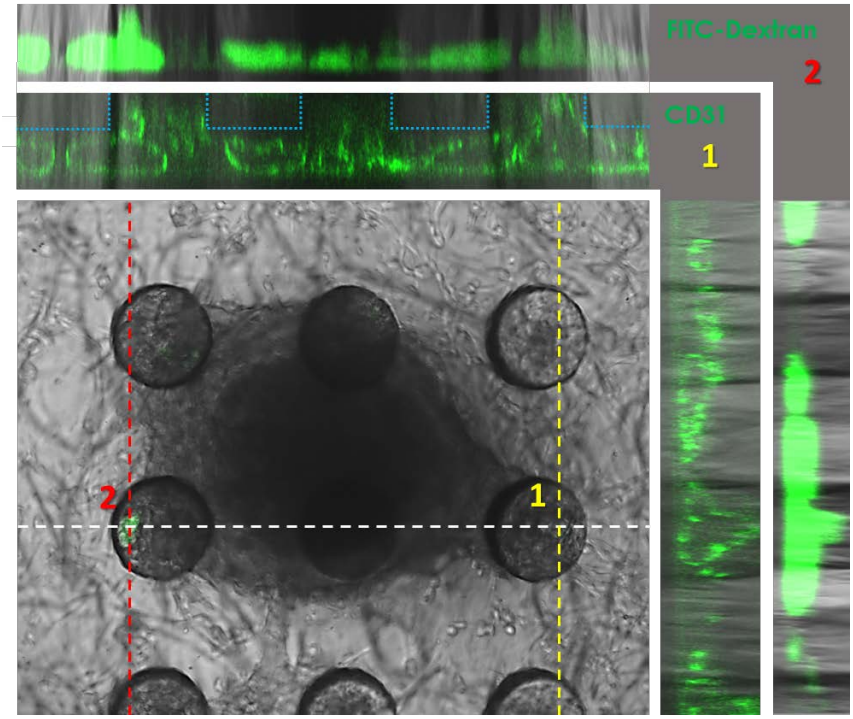


**Figure 3.14** Yellow dotted line indicate where the spheroid is and microvessel lumen are thick enough to flow green dyes right underneath the spheroid. Position 1 is immuno-stained microvessel with CD31. Clear lumen and vessel sprouts vertically directed is observed. Position 2 is cross section image of microvessel filled with FITC-dextran. Dyes are observed filling vertical sprout direction.

## 3.4 Conclusion

Here in this chapter, we have successfully designed device useful to co-culture micro and macro sized system. Here, micro-structures are precisely embedded in the device and help to culture cells in three dimensional space and provide tunnel to microvessel and cell spheroid. To fabricate the monolithic device with both pores and posts, reversed imaged of microchannel pre-mold is fabricated in photolithography. While the photolithography, first layer with holes become posts part of PDMS pre-mold, and second layer with posts become holes part of PDMS pre-mold at the same time. Therefore, thickness of the channels and embedded membranes are determined at this point. If first layer is coated thicker than 75 μm, the thickness of micro pore become thick. Pre-mold is coated with Teflon to prevent fusion with added PDMS. Removal of pre-mold creates thin PDMS membrane with micro pores and micro posts. And this membrane is bonded with PDMS piece with reservoirs.

With the device, we have successfully cultured microvessel. Also, the vessel is compared with control, which the channel is not vertically opened. Therefore, we observed the thicker microvessel lumen with

micro pore embedded device.

Then the device is tested by selectively flowing fluids either through vessel or outside vessel. Well connected and perfused microvessel can maintain the different fluid condition over 30 minutes. Dyes could not diffuse out or in through the vessel wall. This is big advantage of the device because it can possibly provide two types of media cultured in the same device blocked just with biological barrier. This refers to natural condition in our body where tissues and vessels are merged together. With this character, we have tested the device with two type of media and observed the microvessel difference after two days. We were able to distinguish the result among selected samples.

Finally, we have co-cultured with cancer spheroid on top of the vascular network. Size of cancer spheroid is around 300~500 μm however, larger system can be used as the size of open top reservoir is 6 mm in diameter. Also, the pore size can be managed up to 500 μm which can increase chance to contact with co-cultured tissue. By co-culturing microvessel with cancer spheroid, we were able to observe the difference of microvessel behavior. As U87MG can plentiful VEGF factors, microvessel can increase their vessel thickness, complex network and

aligning their growth direction. Further we have witnessed the vertical sprouting towards the cancer spheroid which would not be possible without the presence of micro pores.

Here we wanted to created microfluidic device with open access to vascular network assembled within the device. Inner and exterior side of lumen is approachable at any time which is novel advantage of the platform. Through “Open-top”, we were able to deliver sufficient media supply to every corner of wide channel. Different with conventional membrane, the micropore is designed large enough for cell spheroid to settle down and enables direct contact with cell complex lower channel. As the device can feature spatial culture, it can be compared to capillary bed complex in our body. Also we have observed selected fluid delivery. We estimate excellent potential to this platform and expect this device to be used as a new breakthrough of science technology beyond tissue engineering.

# 4 Micro Blood Vessel Module (μBVM) for Organ-on-a-Chip Applications

## 4.1 Introduction

### 4.1.1 Circulatory system and human-on-a-chip

The circulatory system is an organ system where blood circulates the whole body from top to bottom transporting vital materials such as nutrients, oxygen, carbon-dioxide, hormone, and cells. Blood vessel network that has spread to every corner of our body flows from vein to artery powered from pumping heart connecting tissues and organs. This being so, when developing treatments or investigating biological theories about certain organs, researchers will have to consider not only target organ but also interacting organs. Because one organ never function alone. In chapter 1 introduction, we have introduced few developed organ-on-a-chip models which better simulate in vivo conditions using microfluidic devices. Each models are novel enough to represent key functions of its organs. However, considering the organ networks in our body, efforts to connect these models as “Human-on-a-chip” is studied in few laboratories [20, 21]. Here in this last chapter, we introduce simple method to engineer perfusable networks of blood vessels that can serve as a module to connect several organ components as a part of body-on-a-chip applications.

### 4.1.2 Idea of hydrogel loop insert

The key of μBVM is; i) be simple, ii) be easy for applications, and iii) be a microchip only with blood vessel. First, in order to assemble blood vessel network in microfluidic device, always the “cell” is the important factor. We use fibroblast to secrete growth factors for endothelial cells to differentiate and assemble into microvessel. To obtain microchip only with blood vessel, we need to somehow remove fibroblast after their work is done. The idea of hydrogel loop comes from tea infuser. We need a tool to soak fibroblasts for secretion and extract them easily, similar as transwell. Transwell is useful tool to culture two type of cells communicating each other but prohibit physical contact. But conventional transwell is too large for microfluidic device. Therefore we thought of using disposable inoculating loop with 10 μl volume. As the diameter is less than 7 mm, it can possibly fit in reservoirs connected to microfluidic channels. Inner loop can hold hydrogel up to 20 μl, so that we were able to trap number of fibroblast enough to deliver growth factors. The idea of hydrogel loop insert, it have many potential as it can capture any type of cells on demand. Researchers can simply insert and remove or replace cells in concern observing effect with vascular networks.

### 4.1.3 Aim of the paper

Here we have designed a millimeter-scale perfusable network of blood vessels that can serve as a module to connect various organ components as a part of human-on-a-chip applications. Successful assembly of the vessel network was helped by the using hydrogel loop insert which is O-ring shaped containing 3D cultured lung fibroblasts (LFs) in hydrogel. Within the loop, LFs are physically isolated however free to secrete growth factors so that endothelial cells (ECs) can differentiate. We could obtain perfusable micro-capillary vessels that were composed only with endothelial cells after the vessel formation by simply removing LF loop. As the cells have low chance to contaminate each other by close contact, clear vessel opening is observed between micro posts. The module has a single microchannel with an inlet-outlet pair, and it is thus able to support the connections with other organs and can represent a system that mimics blood circulation. Therefore, we expect this microscale blood vessel module (μBVM) to be used as a functional module of future body-on-a-chip platforms.

## 4.2 Material and Method

### 4.2.1 Fabrication of the Microchannel

A microfluidic device was fabricated using soft lithography and other published techniques. Briefly, a plasma-treated silicon wafer was spin-coated with 150 μm thick negative photoresist, SU-8 100 (MicroChem, Boston, MA). After prebaking at 65 °C for 10 min and 95 °C for 30 min, the wafer was exposed to 405 nm ultraviolet (UV) light (Shinu MST, Gyeonggi-do, Korea) for 500 mJ. After the exposure, the wafer was baked at 65 °C for 1 min and 95 °C for 10 min. SU-8 developer (Microchem) was used to remove the unexposed part of the photoresist. Using this wafer as the master mold, PDMS precursor Sylgard 184 (Dow Corning, Midland, MI) was poured, baked, and replicated. After punching for the inlets and reservoirs, the PDMS block was attached on the coverslip by plasma treatment (Femto Science, Gyeonggi-do, Korea). The attached device was heated on the 80 °C dry oven overnight to turn the surfaces hydrophobic**.**

### 4.2.2 Cell Culture

HUVECs (Lonza, Basel, Switzerland) were cultured in the endothelial growth medium (EGM-2; Lonza), and cells between passages 4 to 5 were used.

Primary human LFs (Lonza) were cultured in fibroblast growth medium (FGM-2; Lonza), and passages 6 to 10 were used for the experiment. To harvest the cells, they were rinsed with phosphate buffered saline (PBS) and treated with 0.25% trypsin–EDTA (Gibco, Carlsbad, CA). After 2 min, M199 (Lonza) containing 10% fetal bovine serum was added to neutralize the effect of the enzyme. Detached cells were collected and centrifuged for 2 min in 1100 rpm, and diluted in EGM-2 to reach a certain cell number in the suspension.

### 4.2.3 LF–Hydrogel Loop Preparation

A plastic loop (Loop and Needle, SPL Life Science, Gyeonggi-do, Korea) was trimmed and used for capturing the LF–fibrin mixture (Figure 4.1). LFs were cultured and harvested from a tissue culture dish, and they were suspended in EGM-2 to 2.5~4×$10^6$cells/ml. Bovine fibrinogen solution (2.5 mg/ml fibrinogen with 0.15 U/ml approtinin) was added to the cell suspension, and the LF-containing hydrogels were mixed with thrombin (0.5 U/ml) immediately before loading on the inside loop portion. A total of 20 μl LF-containing hydrogels was then gently suspended at the inner surface of the plastic loop. After placing the gel-loaded loop into a 96-well plate, it was allowed to gel for 5 min. When the gels solidified, 200 μl of medium was filled and incubated for a day before use.

### 4.2.4 Live/Dead Assay

A live/dead assay kit (Molecular Probes L3224; Invitrogen, Carlsbad, CA) was used quantify LF viability when cultured in a hydrogel loop. The LF loop was gently rinsed with PBS and dipped into antibodies for 30 min. Hoechst 33342 was used to stain the nucleus. The LF loop was then rinsed with PBS and prepared for fluorescent imaging. Fluorescent images were taken with the confocal microscope FV1000 (Olympus, Tokyo, Japan) with a 3 μm interval. Stacked images were then deconvoluted into a 3D image using IMARIS (Bitplane, Zurich, Switzerland).

### 4.2.5 Preparation of μBVM

Fibrinogen was prepared as described above. HUVEC was mixed with the fibrinogen and injected into the microchannel. Mixture fluid was placed only in the microchannel because of the surface tension at the edge of the hydrophobic microchannel, which prohibits the further progress of the fluid. After 5 min incubation at room temperature to solidify the hydrogel, the fresh medium was added. The LF loop was then dipped into each reservoir to let HUVECs differentiate. The fresh medium was changed every 2 days.

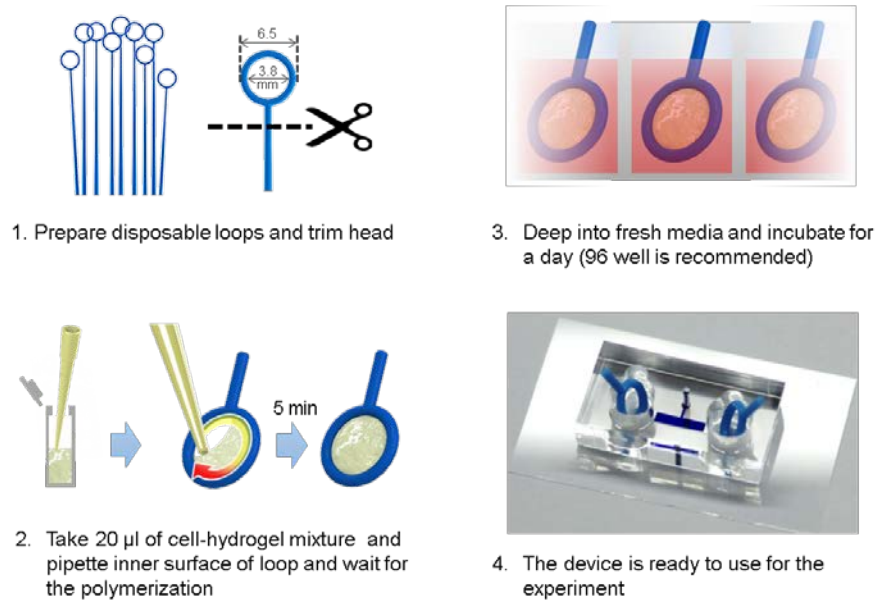


**Figure 4.1** Schematic showing the preparation of a hydrogel loop. The figure showes each steps to prepare hydrogel loop. Loop is trimmed from conventional cell spreader and premixed hydrogel containing cells are pipetted inner surface of the loop. Hydrogel loop is incubated in the 96 well before use. Each loop is inserted into reservoir of the device secreting growth factor. Hydrogel boundaries prevent cells from crawling out of the loop. Hydrogel loop can be freely removed or exchanged with other loop.

### 4.2.6 Immunostaining and Imaging of the Capillary

To configure the physiological relevance of the blood vessel, samples were fixed with 4% paraformaldehyde. They were permeabilized with 0.15% Triton X-100 for 15 min and treated with PBS solution containing 3% bovine serum albumin (BSA; Sigma-Aldrich, St. Louis, MO). To visualize the lumens of the blood vessel, green fluorescent protein–conjugated Phalloidin (Molecular Probes) was used with a ratio of 1:200, and Hoechst 33342 for the nucleus (1:1000). Fluorescent images of the capillary were taken with the confocal microscope with every 3 μm height. The stacked images were deconvoluted into 3D volume using IMARIS.

## 4.3 Results and discussions

### 4.3.1 Loop–Hydrogel Culture of the Lung Fibroblast in μBVM

For the sustained secretion of growth factor from LFs, verification of the loop culture was conducted. We have tested the loop sample with the live/dead assay and compared their viability while they were at 1 and 10 days in vitro (Figure 4.2 C). Live and dead cells were distinguished by counting the cell nuclei. Over 95% of the fibroblast appeared alive after 10 days in hydrogel. Referring no significant difference to DIV1. The total number of cells can be controlled because the maximum amount of the hydrogel cell cocktail depends on the size of the diameter of the loop. We have counted $2.5\sim4\times10^{6}$cells/ml in the hydrogel mixture, and the loop (3.8 mm inside diameter) holds up to 20 μl. referring to previous publications, LFs in the channel counted 30,000, which is half of the amount of ours. However, we have experienced that a higher concentration of LFs induced detachment of hydrogel from the loop surface, resulting in a non-uniform distribution of cells.

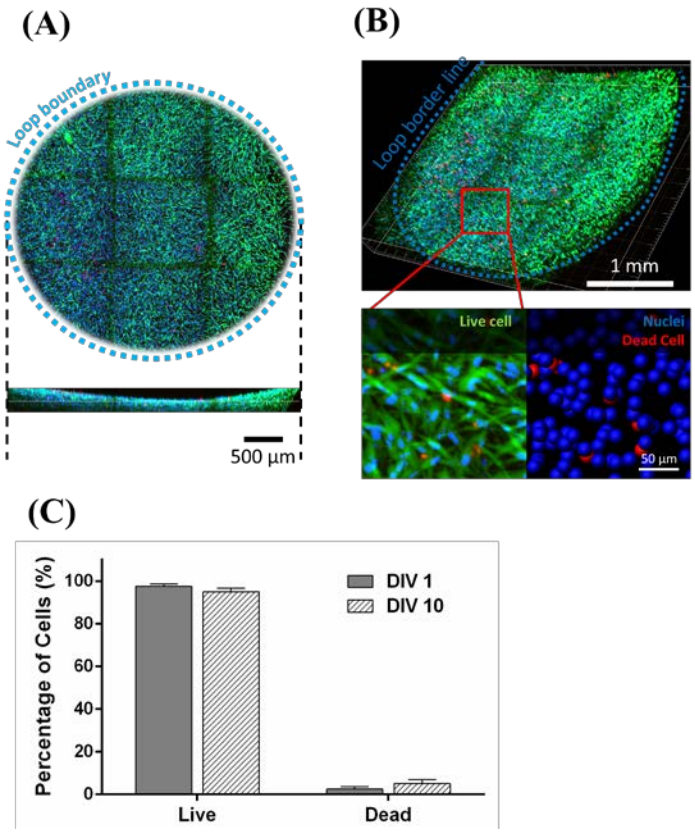


**Figure 4.2** Live/dead assay is performed to verify cell viability. (A) Cells are uniformly distributed within hydrogel. Loop boundary keep cell from escaping and prevent cell interference. (B) Live/dead assay is performed for cells in hydrogel loop. Cells are well cultured during 10 days in vitro. Nuclei of the cells are reconstructed with IMARIS and counted by their color. Blue sphere stands for live cells while red sphere are dead cells. (C) Graph shows that a high percentage of cells (95%) remains viable within the gel for up to 10 days referring no significant difference to DIV 1.

### 4.3.2 Verification of Blood Vessel Formed in μBVM

Blood vessels, the most important conduit for organs, were recently engineered in a microfluidic platform. In the previous research of our group, we have reported that co-culturing of LFs and ECs in a defined hydrogel microenvironment could induce the perfusable blood vessel network. This work was different in a few ways from previous works that used preformed tubes in hydrogel whose inner surface was coated with endothelial cells. First, our vessels showed tighter cell–cell junction and thus lower permeability. When endothelial cells coated the inner surface of a tube, it took some time for the cells to proliferate and eventually form a completely covered monolayer. In this approach, there may be some local areas where the cell–cell junctions do not close completely or do not mature enough to form a tight barrier. Second, the vessels in this work were formed naturally rather than coated on an artificially formed single tube. Therefore, the diameter was not controlled by the diameter of the tube but by the origin of the endothelial cells themselves. These factors made it more physiologically relevant. In this research, to make a functional unit blood vessel, we introduced transferrable loop cultured fibroblast instead of a predefined microfluidic device. Benefits of the co-culture were obtained by simply dipping the loop with fibroblast in the medium reservoirs. Due to the biomolecules that were secreted from the loop, a perfusable blood vessel was formed. The loop could prevent LFs from interrupting the ECs. This offered a

big advantage because the previous design had to suffer from cell-to-cell contamination. HUVECs were observed day by day (Figure 4.3 A). Within 10 days, we could observe perfused blood vessels throughout the channel. Here, we designed a 2 mm length vessel channel, which was decided to be an appropriate dimension. Our experiments had been performed for up to 4.5 mm length. We could observe the EC differentiation throughout the long channel, but the center region had a relatively smaller amount of growth factors supplied compared to the inlet and outlet. That resulted in an open vessel in the channel access and flat lumen in the middle, inhibiting full perfusion of the vessel. After the blood vessel formation, we have immunostained μBVM to visualize the lumens. 7 μm of red fluorescent micro bead was introduced in the reservoir to visualize the perfusability (Figure 4.3 B). Because the blood vessel was induced by a physically separated hydrogel loop, we were able to decouple the LF loop. However, without growth factors responsible for blood vessel maturation, removal of the hydrogel loop leads to disassembly of the lumen within a day. Further experiments to stabilize the blood vessel without LFs can be researched with μBVM because this is the first model supporting transferable culture.

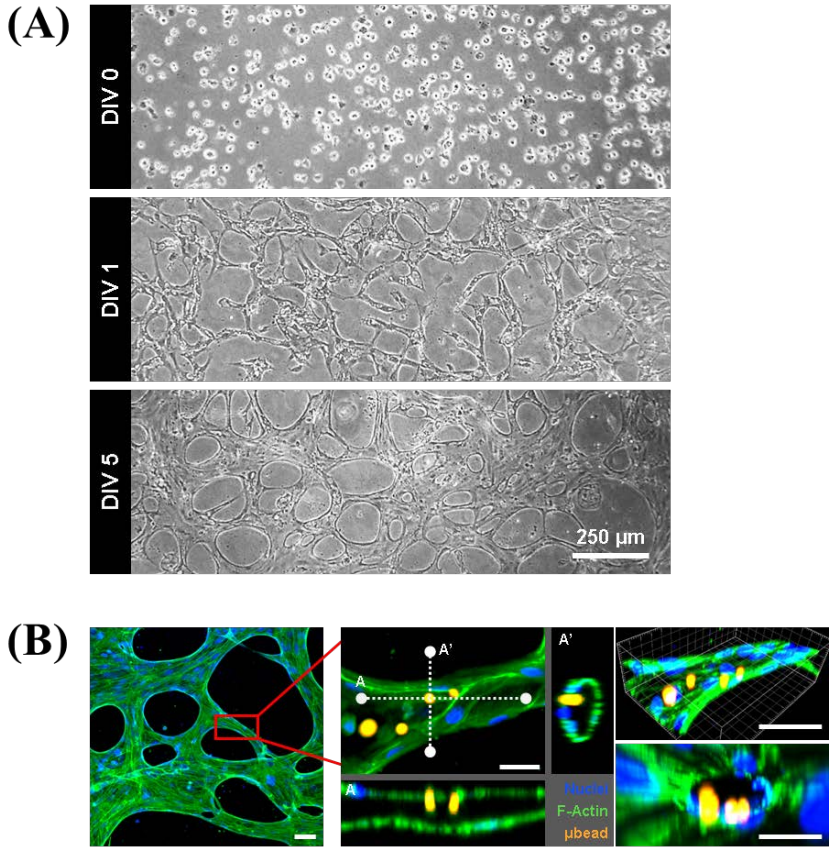


**Figure 4.3** (A) Bright-field images of HUVECs forming a capillary vessel inside of the microchannel were captured from day to day. Morphology of the HUVEC is observed. Maximum channel length to maintain perfusability is 2 mm. (B) Immuno-stained μBVM. μBVM is stained to visualize vessel network and interior lumen. 7 um red fluorescent beads are introduced from the reservoir to verify perfusability. Scale bar shows 50 μm.

### 4.3.3 Extended μBVM for Organ-on-a Chip

By changing the cell types captured in a hydrogel loop, the source of paracrine factors exposed to the blood vessel could be changed. This process may lead to the design of further study to reveal interactions between blood vessels and other distinct cells or tissues. A hydrogel loop can be used as a method to decouple the presence of other cell types regarding the paracrine effect, which would be helpful for tissue and organ models in microfluidics research. We have described the connected reservoirs of the μBVM in serial (Figure 4.4A). With this strategy, we could handle multiple culture dishes connecting through the perfusable blood vessel. This extended μBVM could connect multiple in vitro human tissues or organ models with biologically induced blood capillaries. As a body-on-a chip platform, previous research had suggested the endothelial-coated conduit. However, after creating a naturally induced blood vessel, we expect to observe the feedback interaction with the blood conduit in more in-vivo-like circumstances, especially for perspectives on permeability.

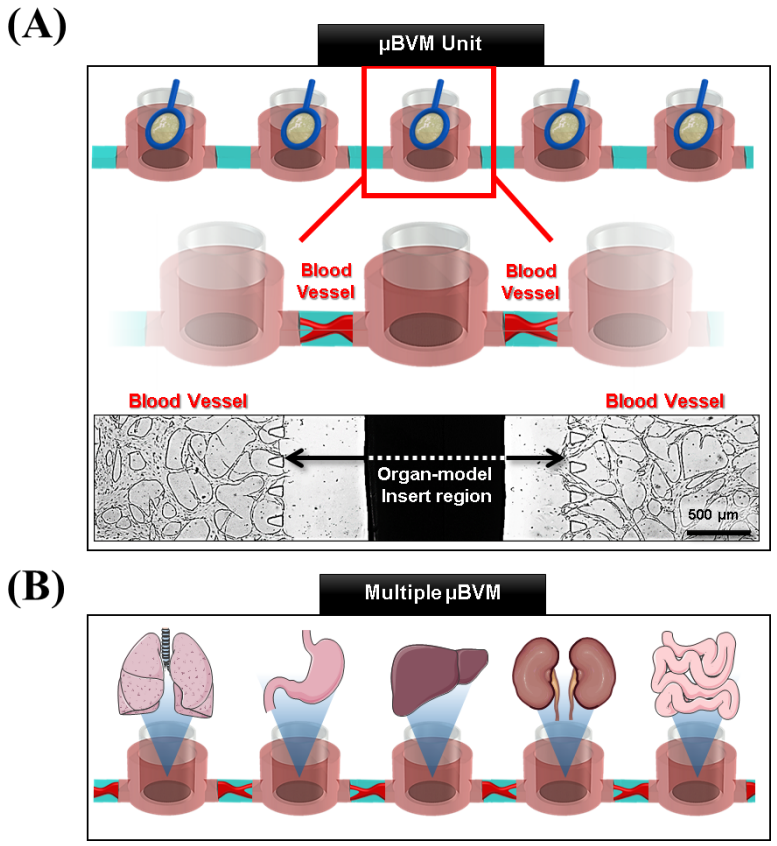


**Figure 4.4** (A) Bright field image of connected two units of μBVM. Center insert region is allowed to insert organ representing cell types into microfluidic device with only containing micro-blood vessel. (B) Cells in Hydrogel loop can be decoupled from cells in the device after they spend enough time to affect each other. This is one of big advantage of the μBVM system. By culturing any cell types in hydrogel loop and exchange, this can be another cell secreting source.

## 4.4 Conclusion

Here in this chapter, we propose a modular blood vessel platform with a simple microchannel design that can be engineered with a paracrine factor secreting hydrogel loop. LFs were captured within a hydrogel loop by surface tension and placed around the HUVEC-laden microchannel, inducing blood vessel formation between the loops. By loading a high density of LFs into the removable loop, “long” blood vessels on the order of a few millimeters were formed between the loops by paracrine factors. When placed in series, the cell-laden loops can form blood vessels that can further function as modular connectors between different compartments. After the vessels are formed, the μBVM loops can be replaced with organ-on-a-chip devices, thus forming a conduit between different organs on a body-on-a-chip device.

# 5 Conclusion

This paper introduces platforms in double layered structure in order to successfully perform their experimental purpose. Basically the models are improved from original microfluidic blood vessel platform. Therefore the devices share common characters and also have their distinct features (Figure 5.1). To briefly introduce the original device, it performs natural assembly of blood vessel. The device is widely used to many different types of experiments. The device is stable, reliable and easy to use. However, it had few limitations that since the channels have closed boundaries except the gap between the posts, the device is difficult to assemble longer blood vessel channel. Also, the height of the device is less than 150 μm so that the small tissues cannot be accessed within the device.

By improving the device, we were able to overcome the difficulties and proceed experiments which only our platforms could perform. Splitting channels in vertical direction allowed additional access to vessel channel and we were able to deliver fluids to exterior side of the microvessel. Therefore, Platform #1 is used to evaluate the effect of chemical reagent to blood vessel in high manner of resolution which was difficult in other assays. And Platform #2 can feature similar with capillary bed because they have vascular culture region as well as tissue culture region. From enough media perfusion through

additional inlets, longer and larger area of vascular networks can be formed. With the device, we have co-cultured with cancer spheroid. Here we have only performed co-culture just with the cancer spheroid, however the device have unlimited potential to be applied with other type of tissues. For example, considering the spatial context of the device, reconstructed skin tissue can be cultured on top of the vascular networks. As introduced in chapter 2, skin model with microvessel is still on research and is everybody's demand. As dermis is complexed with capillary vessels, it would be a good start to begin with.

To conclude the paper, we have designed novel microfluidic device which is useful and possess many possibilities. We estimate excellent potential to all of these platforms and expect these platforms to be used as a new breakthrough of science technology beyond tissue engineering.

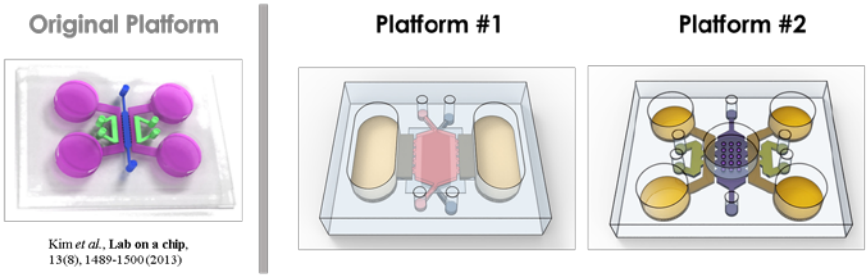


| Original Platform | Criteria | Platform#1 | Platform#2 |
|---|---|---|---|
| O | Blood vessel formation | O | O |
| O | Co culture with other cells | O | O |
| X | Co culture with spheroid or small tissue | X | O |
| X | Media perfusion | O | O |
| X | Longer vessel formation (1 mm ~) | △ | O |
| X | Chemical from external side of blood vessel | O | O |
| O | User friendly | X | X |

**Figure 5.1** Advantage and disadvantage of the devices. Platform # 1, 2 is integrated from original platform and have an improved points. Important criteria is listed and each platform ability is compared.

# 6 Reference


[1] G. M. Whitesides, "The origins and the future of microfluidics," *Nature,* vol. 442, pp. 368-73, Jul 27 2006.

[2] J. El-Ali, P. K. Sorger, and K. F. Jensen, "Cells on chips," *Nature,* vol. 442, pp. 403-11, Jul 27 2006.

[3] S. K. Sia and G. M. Whitesides, "Microfluidic devices fabricated in poly(dimethylsiloxane) for biological studies," *Electrophoresis,* vol. 24, pp. 3563-76, Nov 2003.

[4] S. Haeberle and R. Zengerle, "Microfluidic platforms for lab-on-a-chip applications," *Lab Chip,* vol. 7, pp. 1094-110, Sep 2007.

[5] A. L. Paguirigan and D. J. Beebe, "Microfluidics meet cell biology: bridging the gap by validation and application of microscale techniques for cell biological assays," *Bioessays,* vol. 30, pp. 811-21, Sep 2008.

[6] J. H. Yeon and J. K. Park, "Microfluidic Cell Culture Systems for Cellular Analysis," *BIOCHIP,* vol. 1, pp. 17-27, 2007.

[7] S. Halldorsson, E. Lucumi, R. Gomez-Sjoberg, and R. M. Fleming, "Advantages and challenges of microfluidic cell culture in polydimethylsiloxane devices," *Biosens Bioelectron,* vol. 63, pp. 218-31, Jan 15 2015.

[8] A. M. Taylor, M. Blurton-Jones, S. W. Rhee, D. H. Cribbs, C. W. Cotman, and N. L. Jeon, "A microfluidic culture platform for CNS axonal injury, regeneration and transport," *Nat Methods,* vol. 2, pp. 599-605, Aug 2005.

[9] B. Vahidi, J. W. Park, H. J. Kim, and N. L. Jeon, "Microfluidic-based strip assay for testing the effects of various surface-bound inhibitors in spinal cord injury," *J Neurosci Methods,* vol. 170, pp. 188-96, May 30 2008.

[10] A. N. Hellman, B. Vahidi, H. J. Kim, W. Mismar, O. Steward, N. L. Jeon, *et al.*, "Examination of axonal injury and regeneration in micropatterned neuronal culture using pulsed laser microbeam dissection," *Lab Chip,* vol. 10, pp. 2083-92, Aug 21 2010.

[11] S. Hosmane, A. Fournier, R. Wright, L. Rajbhandari, R. Siddique, I. H. Yang, *et al.*, "Valve-based microfluidic compression platform: single axon injury and regrowth," *Lab Chip,* vol. 11, pp. 3888-95, Nov 21 2011.

[12] J. W. Park, H. J. Kim, M. W. Kang, and N. L. Jeon, "Advances in microfluidics-based experimental methods for neuroscience research," *Lab Chip,* vol. 13, pp. 509-21, Feb 21 2013.

[13] P. J. Lee, P. J. Hung, and L. P. Lee, "An artificial liver sinusoid with a microfluidic endothelial-like barrier for primary hepatocyte culture," *Biotechnol Bioeng,* vol. 97, pp. 1340-6, Aug 1 2007.

[14] K. J. Jang, A. P. Mehr, G. A. Hamilton, L. A. McPartlin, S. Chung, K. Y. Suh, *et al.*, "Human kidney proximal tubule-on-a-chip for drug transport and nephrotoxicity assessment," *Integr Biol (Camb),* vol. 5, pp. 1119-29, Sep 2013.

[15] D. Huh, D. C. Leslie, B. D. Matthews, J. P. Fraser, S. Jurek, G. A. Hamilton, *et al.*, "A human disease model of drug toxicity-induced pulmonary edema in a lung-on-a-chip microdevice," *Sci Transl Med,* vol. 4, p. 159ra147, Nov 7 2012.

[16] H. J. Kim, D. Huh, G. Hamilton, and D. E. Ingber, "Human gut-on-a-chip inhabited by microbial flora that experiences intestinal peristalsis-like motions and flow," *Lab Chip,* vol. 12, pp. 2165-74, Jun 21 2012.

[17] H. E. Abaci, K. Gledhill, Z. Guo, A. M. Christiano, and M. L. Shuler, "Pumpless microfluidic platform for drug testing on human skin equivalents," *Lab Chip,* vol. 15, pp. 882-8, Feb 7 2015.

[18] S. N. Bhatia and D. E. Ingber, "Microfluidic organs-on-chips," *Nat Biotechnol,* vol. 32, pp. 760-72, Aug 2014.

[19] D. Huh, G. A. Hamilton, and D. E. Ingber, "From 3D cell culture to organs-on-chips," *Trends Cell Biol,* vol. 21, pp. 745-54, Dec 2011.

[20] M. A. Guzzardi, F. Vozzi, and A. D. Ahluwalia, "Study of the crosstalk between hepatocytes and endothelial cells using a novel multicompartmental bioreactor: a comparison between connected cultures and cocultures," *Tissue Eng Part A,* vol. 15, pp. 3635-44, Nov 2009.

[21] I. Wagner, E. M. Materne, S. Brincker, U. Sussbier, C. Fradrich, M. Busek, *et al.*, "A dynamic multi-organ-chip for long-term cultivation and substance testing proven by 3D human liver and skin tissue co-culture," *Lab Chip,* vol. 13, pp. 3538-47, Sep 21 2013.

[22] S. Kim, H. Lee, M. Chung, and N. L. Jeon, "Engineering of functional, perfusable 3D microvascular networks on a chip," *Lab Chip,* vol. 13, pp. 1489-500, Apr 21 2013.

[23] J. A. Whisler, M. B. Chen, and R. D. Kamm, "Control of perfusable

microvascular network morphology using a multiculture microfluidic system," *Tissue Eng Part C Methods,* vol. 20, pp. 543-52, Jul 2014.

[24] N. L. Parenteau, C. M. Nolte, P. Bilbo, M. Rosenberg, L. M. Wilkins, E. W. Johnson, *et al.*, "Epidermis generated in vitro: practical considerations and applications," *J Cell Biochem,* vol. 45, pp. 245-51, Mar 1991.

[25] Y. Poumay, F. Dupont, S. Marcoux, M. Leclercq-Smekens, M. Herin, and A. Coquette, "A simple reconstructed human epidermis: preparation of the culture model and utilization in in vitro studies," *Arch Dermatol Res,* vol. 296, pp. 203-11, Oct 2004.

[26] Y. Poumay and A. Coquette, "Modelling the human epidermis in vitro: tools for basic and applied research," *Arch Dermatol Res,* vol. 298, pp. 361-9, Jan 2007.

[27] F. Netzlaff, C. M. Lehr, P. W. Wertz, and U. F. Schaefer, "The human epidermis models EpiSkin, SkinEthic and EpiDerm: an evaluation of morphology and their suitability for testing phototoxicity, irritancy, corrosivity, and substance transport," *Eur J Pharm Biopharm,* vol. 60, pp. 167-78, Jul 2005.

[28] C. Tornier, M. Rosdy, and H. I. Maibach, "In vitro skin irritation testing on reconstituted human epidermis: reproducibility for 50 chemicals tested with two protocols," *Toxicol In Vitro,* vol. 20, pp. 401-16, Jun 2006.

[29] K. R. Mewes, M. Raus, A. Bernd, N. N. Zoller, A. Sattler, and R. Graf, "Elastin expression in a newly developed full-thickness skin equivalent," *Skin Pharmacol Physiol,* vol. 20, pp. 85-95, 2007.

[30] M. Schafer-Korting, A. Mahmoud, S. Lombardi Borgia, B. Bruggener, B. Kleuser, S. Schreiber, *et al.*, "Reconstructed epidermis and full-thickness skin for absorption testing: influence of the vehicles used on steroid permeation," *Altern Lab Anim,* vol. 36, pp. 441-52, Sep 2008.

[31] L. Gibot, T. Galbraith, J. Huot, and F. A. Auger, "A preexisting microvascular network benefits in vivo revascularization of a microvascularized tissue-engineered skin substitute," *Tissue Eng Part A,* vol. 16, pp. 3199-206, Oct 2010.

[32] T. Uchino, T. Takezawa, and Y. Ikarashi, "Reconstruction of three-dimensional human skin model composed of dendritic cells, keratinocytes and fibroblasts utilizing a handy scaffold of collagen vitrigel membrane," *Toxicol In Vitro,* vol. 23, pp. 333-7, Mar 2009.

[33] K. J.H. and C. J.C., "Interpretation of eye irritation tests," *Journal of Cosmetic Science,* vol. 13, pp. 281–289, 1962.

[34] P. Gautheron, J. Giroux, M. Cottin, L. Audegond, A. Morilla, L. Mayordomo-Blanco, *et al.*, "Interlaboratory assessment of the bovine corneal opacity and permeability (BCOP) assay," *Toxicol In Vitro,* vol. 8, pp. 381-92, Jun 1994.

[35] J. Folkman and P. A. D'Amore, "Blood vessel formation: what is its molecular basis?," *Cell,* vol. 87, pp. 1153-5, Dec 27 1996.

[36] R. Langer and J. P. Vacanti, "Tissue engineering," *Science,* vol. 260, pp. 920-6, May 14 1993.

[37] M. J. Lysaght and J. Reyes, "The growth of tissue engineering," *Tissue Eng,* vol. 7, pp. 485-93, Oct 2001.

[38] L. G. Griffith and G. Naughton, "Tissue engineering--current challenges and expanding opportunities," *Science,* vol. 295, pp. 1009-14, Feb 8 2002.

[39] K. Y. Lee and D. J. Mooney, "Hydrogels for tissue engineering," *Chem Rev,* vol. 101, pp. 1869-79, Jul 2001.

[40] B. Hendrickx, J. J. Vranckx, and A. Luttun, "Cell-based vascularization strategies for skin tissue engineering," *Tissue Eng Part B Rev,* vol. 17, pp. 13-24, Feb 2011.

[41] D. Marino, J. Luginbuhl, S. Scola, M. Meuli, and E. Reichmann, "Bioengineering dermo-epidermal skin grafts with blood and lymphatic capillaries," *Sci Transl Med,* vol. 6, p. 221ra14, Jan 29 2014.

[42] R. K. Jain, P. Au, J. Tam, D. G. Duda, and D. Fukumura, "Engineering vascularized tissue," *Nat Biotechnol,* vol. 23, pp. 821-3, Jul 2005.

[43] H. Onoe, T. Okitsu, A. Itou, M. Kato-Negishi, R. Gojo, D. Kiriya, *et al.*, "Metre-long cell-laden microfibres exhibit tissue morphologies and functions," *Nat Mater,* vol. 12, pp. 584-90, Jun 2013.

[44] J. H. Yeon, H. R. Ryu, M. Chung, Q. P. Hu, and N. L. Jeon, "In vitro formation and characterization of a perfusable three-dimensional tubular capillary network in microfluidic devices," *Lab Chip,* vol. 12, pp. 2815-22, Aug 21 2012.

[45] H. Lee, S. Kim, M. Chung, J. H. Kim, and N. L. Jeon, "A bioengineered array of 3D microvessels for vascular permeability assay," *Microvasc Res,* vol. 91, pp. 90-8, Jan 2014.

[46] H. Lee, W. Park, H. Ryu, and N. L. Jeon, "A microfluidic platform for quantitative analysis of cancer angiogenesis and intravasation," *Biomicrofluidics,* vol. 8, p. 054102, Sep 2014.

[47] J. Kim, M. Chung, S. Kim, D. H. Jo, J. H. Kim, and N. L. Jeon, "Engineering of a Biomimetic Pericyte-Covered 3D Microvascular Network," *PLoS One*, vol. 10, p. e0133880, 2015.

[48] N. Jusoh, S. Oh, S. Kim, J. Kim, and N. L. Jeon, "Microfluidic vascularized bone tissue model with hydroxyapatite-incorporated extracellular matrix," *Lab Chip*, vol. 15, pp. 3984-8, Oct 21 2015.

[49] K. Sakaguchi, T. Shimizu, S. Horaguchi, H. Sekine, M. Yamato, M. Umezu, *et al.*, "In vitro engineering of vascularized tissue surrogates," *Sci Rep*, vol. 3, p. 1316, 2013.

[50] Y. Liang, X. Y. Li, E. J. Rebar, P. Li, Y. Zhou, B. Chen, *et al.*, "Activation of vascular endothelial growth factor A transcription in tumorigenic glioblastoma cell lines by an enhancer with cell type-specific DNase I accessibility," *J Biol Chem*, vol. 277, pp. 20087-94, May 31 2002.

국문초록

# 세포 공동 배양 및 분석을 위한 이중 구조 미세 유체 플랫폼

오 수 정

서울대학교 대학원 기계전공

본 연구는 다중 규모의 생체 세포들을 공동 배양하고, 분석할 수 있는 이중 구조 미세 유체 플랫폼들을 제시한다. 플랫폼들은 기본적으로 두 층과 중간막으로 이루어져 있다. 본 연구에서 소개 된 플랫폼들은 기존에 가능하지 못했던 다중 규모의 공동 배양을 가능하게 하고, 또한 그를 응용한 물질 분석 및 반응 분석을 할 수 있다.

제 1 플랫폼은 반투과성 중간막으로 인해 0.4 μm 이하의 물질들만 투과할 수 있어서 세포와 같이 구멍보다 큰 물질은 통과할 수 없다. 따라서 첫 번째 층에 구조적으로 관류성 혈관망을 만들 수 있도록 설계하고, 중간막의 아래 층에서 화학물질을 투과시켜 독성평가가 가능한 플랫폼을 구현하였다.

제 2 플랫폼은 중간막에 200 μm 크기의 마이크로 구멍들이 뚫려 있어 아래층과 위층을 연결시켜 준다. 아래층에서는 구조적으로 관류성 혈관망을 형성할 수 있도록 설계하였고, 마이크로 구멍을 통해 혈관망 위에 암세포구 (소조직, 300~500 μm 지름) 를 공동 배양 하였다. 그 결과 암세포에 의한 혈관망의 변화를 볼 수 있었다. 또한

본 플랫폼은 혈관망의 내부에 관류를 할 수 있는 것은 물론이고 혈관망의 외부에서도 물질을 전달 할 수 있도록 해준다. 따라서 혈관의 내부와 외부에 서로 다른 물질을 주입할 수 있고, 이는 생체 내 혈관이 존재하는 환경과 흡사하다고 할 수 있다. 이는 기존의 칩들에서는 가능하지 못했던 부분으로 본 플랫폼이 창의적이라는 것을 나타낸다.

본 연구를 통해 개발 된 플랫폼들은 조직공학, 제약분야 등에서 응용될 수 있다고 보며, 논문에 기재된 실험에 대한 결과를 토대로 더 다양한 분야에서 활용될 수 있도록 본 플랫폼의 발전을 기대하는 바이다.

**주요어: 미세유체소자; 다중규모세포공동배양; 미세혈관; 독성 평가; 모세혈관상**

**학번:** 2012-30923